

DOTTORATO DI RICERCA TOSCANO IN NEUROSCIENZE

CICLO XXXIII

COORDINATORE Prof.ssa Felicità Pedata

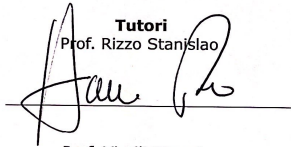
X-linked Retinoschisis: Deep Phenotyping and Genetic Characterization

Settore Scientifico Disciplinare MED/30

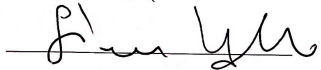
Dottorando
Dott. Finocchio Lucia



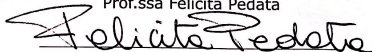
Tutori
Prof. Rizzo Stanislao



Prof. Virgili Gianni



Coordinatore
Prof.ssa Felicità Pedata



Anni 2017/2020

X-linked Retinoschisis: Deep Phenotyping and Genetic Characterization

INDEX

1.INTRODUCTION.....	1
2. MATERIALS AND METHODS.....	11
3. RESULTS.....	15
3.1 CASE REPORTS.....	28
4. DISCUSSION.....	37
REFERENCES.....	I
ACKNOWLEDGEMENTS.....	VII

1. INTRODUCTION

X-linked retinoschisis (XLRS, MIM #312700) is the most frequent inherited degenerative vitreo-retinal dystrophy among young males, accounting for about 5% of all childhood-onset inherited retinal dystrophies, with an estimated worldwide prevalence ranging from 1 in 15,000 to 1 in 30,000. (Molday et al. 2012, Rahman et al. 2020) It is an X-linked recessive disease with almost complete penetrance but with a high degree of intra- and interfamilial variability. (Chen et al. 2014)

XLRS is caused by mutations in the retinoschisin 1 gene (*RS1*, OMIM # 300839) located on the chromosome Xp22.1. (Sauer et al. 1997) *RS1* gene comprises 6 exons and encodes a 224-aminoacid (AA) soluble secretory protein termed retinoschisin (RS) which is produced and secreted as a disulphide-linked homo-ectameric complex, in the extracellular matrix by photoreceptors and bipolar cells, and adheres to their surface. (Molday et al. 2011, Reid et al. 2003, Reid et al. 1999) The RS protein consists of an N-terminal leader sequence characteristic of secreted proteins (exons 1 and 2; 23 AA), a retinoschisin domain (exon 3; 39 AA), a well conserved discoidin domain (exons 4-6; 157 AA) implicated in cell adhesion, and a C-terminal segment (end of exon 6; five AA). The exact function of RS protein is still unknown although it is believed to play an important role in cell adhesion, mediation of cell-to-cell interactions, in maintaining the structural integrity of the retina and the molecular pathway at the photoreceptor-bipolar synapse. (Wu et al. 2005, Ou et al. 2015) More specifically these functions are supported by *RS1* protein structure, which is largely comprised by the discoidin domain (AA residues 62-219), known to facilitate cell adhesion. (Baumgartner et al. 1998) Another proposed role for retinoschisin is the regulation of fluid balance within the photoreceptor and bipolar cell layers, evidenced by the fact that retinoschisin binds to the Na^+/K^+ -

ATPase pump which has a key role in controlling ion gradients and therefore osmolarity. (Molday et al. 2012) Moreover L-type voltage gated calcium channels such as CACNAD1 are supposed to interact with RS1, (Shi et al. 2009) helping to maintain membrane localization of these ion channels and therefore photoreceptor-bipolar cell transmission. (De Silva 2020) *RS1* variants lead to misfolding, misrouting or functional loss of the protein and alteration of normal retinal cells adhesion, resulting in splitting of retinal neural layers and formation of cystoid cavities in the inner nuclear and outer plexiform layers. (The retinoschisis Consortium 1998)

Over 200 disease-causing variants in the *RS1* gene are known with most variants occurring as missense changes identified in exons 4-6, which encode the major protein unit, that is the discoidin domain. (Molday et al. 2012, Renner et al. 2008, Sauer et al. 1997, The retinoschisis Consortium 1998, Pimenides et al. 2005, Riveiro-Alvarez et al. 2009, Bowles et al. 2011, Vincent et al. 2013, Fahim et al. 2017, D'Souza et al. 2013, Gao et al. 2020) Many authors support the fact that there is a profound phenotypic variability, even within families, (Pimenides et al. 2005, Riveiro-Alvarez et al. 2009, Kim et al. 2013, Shinoda et al. 2000, Eksandh et al. 2000, Xiao et al. 2016, Xu et al. 2011) and no clear genotype-phenotype correlations are proven to date. (Gao et al. 2020) Patient with null mutations tend to have more severe XLRS-related visual defects. (Chen et al. 2020)

XLRS can present with diverse clinical and imaging findings. The disease typically presents in the first to second decade with heterogeneous manifestations, including poor visual acuity, strabismus, anisometropia and 'unexplained visual loss', but a smaller number of patients present in infancy with strabismus, nystagmus and/or bullous retinoschisis. (Rahman et al. 2020, George et al. 1995) Visual acuity can vary widely (George et al. 1996) with mean BCVA being 0.49-0.6

LogMAR in recent studies. (Orès et al. 2018, Yang et al. 2014) Fundus examination of the macula reveals the typical macular 'spoke-wheel' folds (macular schisis), fine white dots resembling drusen-like deposits, non-specific retinal pigment epithelium (RPE) changes and macular atrophy, with the latter being seen in older individuals. (De Silva 2020, George et al. 1996, Tsang et al. 2007) Approximately 50% of male adolescent also have peripheral retinal changes, including schisis, metallic sheen (silvery reflex of the internal limiting membrane), pigmentary disturbance, white spiculations, vitreous veils and neovascularization. (Rahman et al. 2020, Vincent et al. 2013, George et al. 1996)

Natural history and prognosis are highly variable even within families. XLRS has a bi-modal presentation. (Grigg et al. 2020) The most frequent one is with a best corrected visual acuity (BCVA) deterioration in the first and second decade (20/60 to 20/120) which coincides with school screening or commencement of school. BCVA typically ranges from 20/50 to 20/120 and may remain stable with a minimal or slow progression until the 5th or 6th decade of life. (Pimenides et al. 2005) Prognosis is often relatively good in childhood. An outer retinal atrophy with resolution of cystic cavities can occur later in adulthood, leading to progressive vision loss (George et al. 1995, Sieving et al. 1993, Gerth et al.2008, Walia et al. 2009). The second less common presentation is with strabismus, vitreous haemorrhage, nystagmus or reduced visual acuity due to peripheral schitic complications frequently before the age of 2 years. (Grigg et al. 2020) During the course of the disease, secondary complications including vitreous or intra-schisis haemorrhage, neovascularization, subretinal exudation, rarely retinal detachment (RD) and traumatic rupture of foveal schisis can occur. Patients with peripheral schisis are at increased risk for high incidence of complications, (Gao et al. 2020)

like recurrent vitreous haemorrhage (VH) and retinal detachment, which are the most frequent events (Fahim et al. 2017). Indeed patients with peripheral retinoschisis, which is seen in 30-71% of patients, develop retinal detachment in 3-16% of eyes (George et al. 1996, Orès et al. 2018). In XLRS, bullous schisis may be congenital or develop soon after birth. It most commonly presents with strabismus. Cases may be complicated by some form of retinal detachment, which may be tractional or a Coats-like exudative detachment. (Hinds et al. 2018)

Early histologic reports localized the region of schisis to the nerve fiber layer. (Yanoff et al. 1968, Manshot et al. 1972) Optical coherence tomography (OCT) allowed to demonstrate macular schisis in the majority of patients, as shown by Orès et al who reports a foveoschisis in 78% of patients and an isolated parafoveal schisis in a further 10%. (Orès et al. 2018) Moreover OCT allows to localize the splitting of the retina with schisis cavities that can be found in any retinal layer, that is within retinal nerve fiber layer (RNFL), ganglion cell layer (GCL), inner nuclear layer (INL), outer plexiform layer (OPL) and outer nuclear layer (ONL), depending on patients age (Eriksson et al. 2004, Gerth et al. 2008, Gregori et al. NZ 2009, Yu et al. 2010). Nevertheless intraretinal cysts can be found predominantly in the INL, followed by the OPL and GCL (Orès et al. 2018). Qualitative changes are also seen in the interdigitation zone, ellipsoid zone and external limiting membrane and photoreceptor outer segments are shorten than controls in XLRS. (De Silva et al. 2020)

The correlations between BCVA and OCT features such as full foveal thickness, photoreceptor thickness and choroidal characteristics have been previously studied with various results. Twenty-five patients with XLRS were evaluated to correlate findings obtained by OCT imaging with VA and macular lesions: there was a lack of

correlation between VA, foveal thickness and cystic area. The anatomical appearance of perifoveal cysts on OCT imaging was most consistent with their location, being primarily within the INL. In older patients, macular cysts were no longer apparent clinically or by OCT imaging, and foveal thickness was reduced. The hypothesis of a primary Müller cell defect was consistent with OCT findings. (Apushkin et al. 2005)

In a retrospective comparative case series, the OCT scans of sixty-three eyes of 33 male patients were analyzed to correlate retinal thickness and volume measurements and correlate these findings with visual acuity and patient age. An increased inner retinal foveal thickness and decreased perifoveal inner retinal thickness were found to correlate with worse visual acuity. Overall retinal thickness decreased with age. (Andreoli et al. 2014) In a retrospective, observational, case-control study, 20 eyes of 10 patients with XLRS were analyzed using Spectral Domain-OCT (SD-OCT) in order to investigate the tomographic characteristics of the outer retinal and choroid and their relationship with visual acuity. Outer plexiform layer and photoreceptor microstructure defects were found to be frequent in XLRS patients. Cone cell outer segment tips line defects may be closely related to poor vision in XLRS. (Yang HS et al. 2014)

In a recent study data from 52 consecutive male patients with XLRS were retrospectively collected in order to analyze the retinal structure using SD-OCT and to correlate the morphologic findings with visual acuity, electroretinographic results and patient age. The study underlined the wide variety of clinical features of XLRS. It highlighted the correlation between visual acuity, patient age, and OCT features, emphasizing the relevance of the latter as potential outcome measure in clinical trials. (Orès et al. 2018)

Swept-source OCT (SS-OCT) and optical coherence tomography angiography (OCT-A) were used to explore the structural features of XLRS in 18 eyes of 9 patients in a retrospective, observational cross-sectional study. The authors found that the hyporeflective spaces on SS-OCT were primarily located at the INL and OPL. Best corrected VA (BCVA) did not correlate with central macular thickness (CMT) or subfield choroidal thickness (SFCT). However external limiting membrane (ELM), ellipsoid portion of inner segment (EPIS) and the cone outer segment tips (COST) defects were significantly correlated with worse BCVA. A positive correlation between age and SFCT was found. (Padron-Pérez et al. 2018)

Handheld SD-OCT images obtained from both eyes of 8 pediatric patients were used to investigate in vivo microanatomic retinal changes and their progression over time in young children with XLRS. SD-OCT findings demonstrated differences in schisis location in fovea-parafoveal versus extrafoveal region, a possible association between poor visual acuity and degree of ellipsoid zone disruption and a decrease in central foveal thickness over time. (Ling KP et al. 2019)

A spoke-wheel pattern of high and low intensity signal represents the characteristic autofluorescent finding in patient with XLRS and it is due to displacement of luteal pigment. (De Silva et al. 2020). Nevertheless recently it has been only identified in approximately half of patients. (Orès et al. 2018, Vincent et al. 2013). Other patterns are represented by normal fundus autofluorescence (FAF), low signal in the foveal region, an area of low signal surrounded by a ring of increased signal intensity, or irregular or regular concentric areas of high- and low-intensity FAF. (De Silva et al. 2020) Over time, FAF can document progression in terms of RPE changes.

The electroretinography (ERG) in XLRS demonstrates a reduced b-to-a amplitude ratio under dark adapted (DA) conditions with a preservation of the a-wave, also known as an 'electronegative ERG'. There is typically light-adapted (LA) 30Hz flicker ERG delay and variable amplitude reduction of the LA ERGs and an implicit time shift at the 30-Hz flicker response under LA conditions. Patients with nonsense, splice-site, or frame-shift variants in *RS1* demonstrate an electronegative DA10 ERG, markedly delayed LA 30Hz (flicker) ERG and an abnormal PERG 50, suggesting some phenotype-genotype correlation (Vincent et al. 2013). Missense variants in *RS1* are characterized by a wider range of ERG abnormalities, including those with the mildest ERG phenotypes; electronegative waveforms are present in most but in a minority the b:a ratio is only mildly reduced. (De Silva et al. 2020) Pattern ERG P50 is usually subnormal in keeping with macular dysfunction but missense changes can be associated with a normal response in a minority. (De Silva et al. 2020, Vincent et al. 2013) Recently the retinal function in young patients with XLRS was assessed: ERG responses to full-field stimuli were recorded under scotopic and photopic condition. Rod and cone photoreceptor and rod-driven post-receptor parameters were calculated from the a- and b-waves. In these young XLRS patients a- and b-wave amplitudes were smaller compared with controls under both scotopic and photopic conditions. The rods' saturated response and a-wave amplitudes were significantly smaller than in controls. Therefore in addition to XLRS causing photoreceptor dysfunction, an effect of XLRS on rod photoreceptors cannot be ignored (Ambrosio et al. 2019).

Female carriers are asymptomatic and there appears to be no clinical disease phenotype, although clinical examination can reveal minor retinal alterations (Kim et al. 2007, Molday et al. 2012). Nevertheless abnormalities in specific

electrophysiological testing protocols in some carriers such as areas of dysfunction on multifocal ERG (Kim 2007) or timing of 8Hz flicker ERG responses (McAnany et al. 2016) have been reported. However a few females have been reported to manifest XLRS, all from consanguineous families and found to have homozygous variants in *RS1* on genetic testing (Ali et al. 2003, Gliem et al. 2014, Rodriguez et al. 2005, Saleheen et al. 2008)

Longitudinal and prospective evaluation of patients with X-linked retinoschisis were performed. Pennesi et al prospectively evaluated 56 patients with XLRS during a 18-month period. They found that structural and functional results were stable during the follow-up. Moreover some patients starting carbonic anhydrase inhibitor treatment at baseline visit showed improvement in BCVA that was not correlated with changes in cyst cavity volume (CCV). (Pennesi IOVS et al 2018)

Cukras et al longitudinally examined the symmetry of structural and functional parameters between the two eyes in 120 males with XLRS, as well as changes in visual acuity and electrophysiology over a 6.8 years. A significant correlation of structural and functional findings between the two eyes and stability of measures of acuity and ERG parameters were demonstrated over time. Their results highlight the utility of the fellow eye as a useful reference for monocular interventional trials. (Cukras IOVS et al. 2018)

There is no specific treatment for XLRS. Carbonic anhydrase inhibitors (CAIs) have been widely used in patients with XLRS with the aim of reducing intraretinal cysts. The effectiveness of topical or oral carbonic anhydrase inhibitor (CAI) on XLRS-associated cystic macular lesions has been shown by using visual acuity, macular thickness on OCT, (Gurbaxani et al. 2014, Collison et al. 2014, Thobani et al. 2011, Genead et al. 2010, Verbakel et al. 2016, Andreuzzi et al. 2017)

microperimetry (MP) and multifocal electroretinogram (mfERG). (Testa et al. 2019)

The most frequently used are topical agents such as dorzolamide. A reduction in intraretinal cysts in 66% of eyes have been reported in the largest study of 36 patients (68 eyes), despite only half the patients maintaining dosing at three times a day. Mean gains in visual acuity were minimal at 0.09 LogMAR. (Andreuzzi et al. 2017) Recently a small mean improvement in visual acuity (3.15 ± 7.8 letters) has been demonstrated in a cohort of patients treated with CAI but with three of 20 subjects showing a >15 letter gain over 18 months follow-up. (Pennesi et al. 2018)

Oral acetazolamide has also been used to treat XLRS. Gurbaxani et al showed a small improvement in visual acuity (0.06 LogMAR) in adults who have been prescribed a dose of 250 mg twice a day in patients over 60 kg (and 125 mg twice a day if under 60 kg). Nevertheless it hasn't been shown a statistically significant reduction in central macular thickness. (Gurbaxani et al. 2014) An improvement in structure on OCT scan and a non-clinically significant improvement in vision was demonstrated in around half of the children treated. (Verbakel et al. 2016) In a recent systematic review (Grigg Eye et al. 2020) 12 studies were evaluated with five series that were natural history observational studies (Jeffrey et al. 2014, Kjellstrom et al. 2010, Cukras et al. 2018, Apushkin et al. 2005, Roesch et al. 1998) and seven that were interventional series using either topical or systemic carbonic anhydrase inhibitors. (Gurbaxani et al. 2014, Apushkin et al. 2006, Andreuzzi et al. 2017, Verbakel et al. 2016, Yang et al. 2013, Khandhadia et al. 2011, Genead et al. 2010)

Visual acuity was found to be the measure most likely to show a statistically significant outcome. The rate of change of vision is slow in most cases in the natural history studies equivalent to 0.22-0.5 letters per year, assuming no peripheral schitic

complications. Macular SD-OCT outcomes were variable depending on cystic changes and showing improvement in CMT but poor correlation with VA.

XLRS is particularly attractive as a target for gene therapy because mutations are in a single gene, RS1, and the preclinical studies in Rs1-knockout (KO) mouse showed rapid treatment benefit to both retinal structure and function. In particular a functional ERG improvement was obtained after intravitreal RS1 gene replacement in knockout mice. (Ou et al. 2015, Byrne et al. 2014) After that, two phase I/II XLRS gene therapy trials delivering gene replacement intravitreally (NCT02416622 run by Applied Genetics Technology Corp (AGTC) and NCT02317887 run by National Eye Institute [NEI]) started and both use an intravitreal approach: the former has been ceased due to marked ocular inflammation while the latter has added additional agents to the standard oral steroids used in subretinal gene supplementation trials to address the uveitis adverse events. (Cuckras et al. 2018, Rahman et al. 2019)

It's imperative to understand the natural progression of the disease and to perform a precise phenotypic characterization when choosing outcome measures to monitor disease progression and outcomes of therapeutic interventions. Herein we examined the clinical characteristics, the structural and functional outcomes in the largest XLRS cohort reported in the literature, consisting of 132 molecularly confirmed children and adults. In particular, we aim to describe their genetic and clinical features and to longitudinally establish clinical correlations between BCVA and age, OCT characteristics, FAF features and complications at baseline and over time. Moreover we aim to report any genotype-phenotype correlations.

2. MATERIALS AND METHODS

The study was approved by the Institutional Review Board of the UCL Institute of Ophthalmology and adhered to the tenets of the Declaration of Helsinki. Each subject (and a parent of children <18 years of age) gave written informed before genetic testing. Ethical approval was obtained from Moorfields Eye Hospital for this retrospective single-center observational series.

Subjects

Clinical and ocular imaging data collected in adults and children with XLRS were longitudinally reviewed. XLRS diagnosis was based on clinical findings, family history and confirmed by detection of disease-causing *RS1* variant.

***RS1* Genetic Analysis**

A combination of direct Sanger sequencing and next generation sequencing, including panels of retinal dystrophy genes, whole exome sequencing (WES) and whole genome sequencing (WGS), was used to identify variants in *RS1* gene. All recruited patients were reassessed for their detected variants. Sequence variant nomenclature was obtained according to the guidelines of the Human Genome Variation Society (HGVS) by using Mutalyzer (<https://mutalyzer.nl/>). Classification of all detected variants was also performed based on the guidelines of the American College of Medical Genetics and Genomics (ACMG). (Richards et al. 2015)

Minor allele frequency for the identified variants in the general population was assessed in the Genome Aggregation Database (gnomAD) datasets (<http://gnomad.broadinstitute.org/>). The population data and general coverage by whole-genome sequencing were also provided with the GnomAD database. (<http://gnomad.broadinstitute.org/>). The Combined Annotation Dependent Depletion (CADD) score was calculated for all variants; a score greater than 15 is usually

considered as mildly pathogenic and a score above 20 is strongly indicative. (Rentzsch et al. 2018) General prediction scores were further calculated using MutationTaster (<http://www.mutationtaster.org/>), FATHMM (<http://fathmm.biocompute.org.uk/9>), and REVEL (<https://labworm.com/tool/revel>). Functional prediction was performed employing SIFT (<https://www.sift.co.uk/>), PROVEAN (<http://provean.jcvi.org/index.php>), and Polyphen 2 (<http://genetics.bwh.harvard.edu/pph2/>). Human splicing finder 3.0 (<http://www.umd.be/HSF3/>) was employed for splicing defects prediction. Mammalian (PhyloP30way and PhastCons30way) and vertebrate (PhyloP100way and PhastCons100way) conservation were also investigated. The previously reported variants were surveyed with the HGMD database (<https://portal.biobase-international.com>; accessed on 1st December 2020) and ClinVar (<https://www.ncbi.nlm.nih.gov/clinvar/>).

Ocular Examination and Retinal Imaging

A review of examination records, medical and ocular histories, slit-lamp biomicroscopy and a dilated funduscopy examination were performed. Best-corrected visual acuity (BCVA) was measured using the Snellen charts and converted into logarithm of the minimum angle of resolution (LogMAR) units for statistical analysis. Fundus photography (Optos ultra widefield camera, Optos, Scotland, UK), infrared reflectance (IR), SD-OCT (Spectralis OCT, Heidelberg Engineering, Dossenheim, Germany) and short-wavelength (488-nm) fundus autofluorescence (FAF) were performed at each visit during the follow-up for most of the patients. The presence of complications, such as vitreous haemorrhage (VH) or retinal detachment (RD), were evaluated.

Fundus Autofluorescence

Spectralis OCT was used to obtain high resolution FAF images. The data were registered at baseline and at the last follow-up. We identified four FAF patterns in XLRS patients and the patient were assigned to each group: i) spoke wheel pattern, ii) increased central signal, iii) central reduction in signal, and iv) ring of increased signal (**Figure 1**).

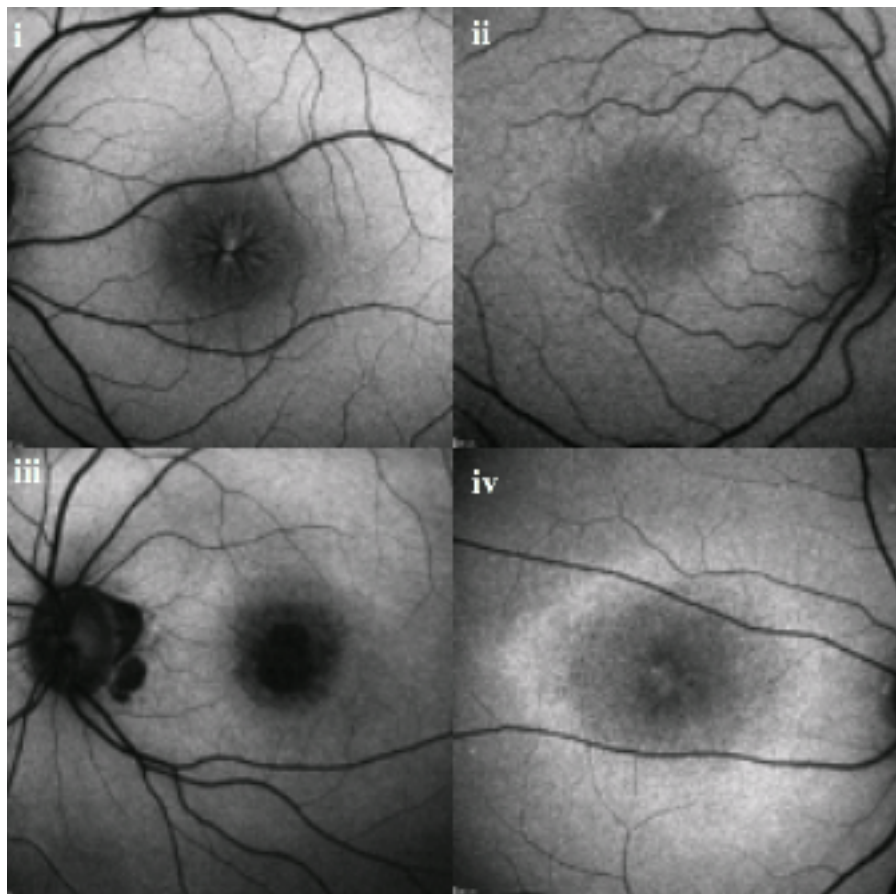


Figure 1: Fundus Autofluorescence Patterns in X-linked Retinoschisis.
i) spoke wheel pattern, ii) increased central signal, iii) central reduction in signal, iv) ring of increased signal.

Optical Coherence Tomography

Spectralis OCT (Heidelberg Engineering, Dossenheim, Germany) was used to obtain high resolution horizontal line scans of the macula in both eyes of the participants. The data were registered at baseline and at the last follow-up. The

presence of foveoschisis, parafoveal schisis and foveal atrophy was evaluated. Schisis localization using vertical and horizontal macular central OCT images was analyzed by evaluating retinal nerve fiber layer (RNFL), ganglion cell layer (GCL), inner nuclear layer (INL), outer plexiform layer (OPL) and outer nuclear layer (ONL). Central macular thickness (CMT) was calculated automatically using a circular ETDRS-type grid positioned on the center of the fovea (central circle of approximately 1-mm diameter that is central subfield), after the scans were reviewed and corrected manually if not appropriate. Defects in the outer retinal photoreceptor microstructures were evaluated, including the interdigitation zone (IZ) and the ellipsoid zone (EZ) in an area 1 mm from the foveal center, also using vertical and horizontal central OCT images. An IZ defect was defined as an irregularity or definite defect of the line. Disruptions in the EZ were defined as signal interruptions at the level of the EZ line for all patients despite a thick schisis. Foveal atrophy was defined as total absence of the IZ or EZ bands. The photoreceptor outer segment (PROS) thickness was calculated by manual measuring of the distance between the EZ and the anterior surface of the retinal pigment epithelium (RPE), as described previously. (Yang HS et al. 2014) The presence of specific OCT findings, including retinal schisis and defects, was determined by consensus between two observers (LF and MG). Any discrepancies between the observers were resolved through discussion with the principal investigator (MM), until consensus was reached.

Statistical Analysis

Statistical analysis was carried out using SPSS Statistics for Windows (Version 22.0. Armonk, NY: IBM Corp.). Significance for all statistical tests was set at $P < 0.05$. The Shapiro-Wilk test was used to test for normality for all variables.

3. RESULTS

Demographic data

In total 132 males from 126 families were ascertained for phenotyping, followed up between 1999 and 2020, in a single tertiary referral center (Moorfields Eye Hospital) in the United Kingdom. One hundred and twenty-seven patients had clinical data and BCVA available at one or more visit. The mean age (\pm SD, range) of the group was 25.4 years old (\pm 16.7, 2.3-70.8 years).

RS1 Genetic Analysis

All recruited patients had likely disease-causing variants in *RS1* gene. In total 66 variants were identified. **Table 1** presents the 12 most frequent variants, and **Figure 2** presents the localization of the identified variants in the gene domains. The five most common variants account for 30.2% of the affected families. Seven variants identified in the cohort are novel (**Table 1**). One variant (c.52+5G>C) was identified in cis with the variant c.35T>A, in three patients, from three different pedigrees, and based on the in silico analysis may not contribute to the disease. **Supplementary Table 1**, presents all sequence variants, based on their HGVS nomenclature and their predicted effect. Missense variants were the most common type of alteration (n=48, 72.7%). Pathogenicity assessment of all detected variants based on the ACMG guidelines, (Richards et al. 2015) are presented in **Supplementary Table 2**. Minor allele frequency, population data and general coverage by whole-genome sequencing for the identified variants in the general population are presented in **Supplementary Table 3**. General prediction scores calculated using MutationTaster (<http://www.mutationtaster.org/>), FATHMM (<http://fathmm.biocompute.org.uk/9>), and REVEL (<https://labworm.com/tool/revel>) are presented in **Supplementary Table 4**. Functional predictions employing SIFT,

PROVEAN, Polyphen 2 and Human splicing finder 3.0 are summarized in **Supplementary Table 5**. Mammalian and vertebrate conservation is presented in **Supplementary Table 6**.

Table 1: Frequent and Novel Variants

c.DNA	Variant (HGVS)*		Patients (n=)	Pedigrees (n=)	Patients (%)	Pedigrees (%)
		Protein				
Frequent Variants						
c.304C>T		p.(Arg102Trp)	10	10	7.6%	7.9%
c.574C>T		p.(Pro192Ser)	8	8	6.1%	6.3%
c.214G>A		p.(Glu72Lys)	8	7	6.1%	5.6%
c.598C>T		p.(Arg200Cys)	7	7	5.3%	5.6%
c.35T>A†		p.(Leu12His)	6	6	4.5%	4.8%
c.421C>T		p.(Arg141Cys)	5	5	3.8%	4.0%
c.(?_1-1)_(52+1_53-1)del		p.(=)	4	4	3.0%	3.2%
c.305G>A		p.(Arg102Gln)	8	4	6.1%	3.2%
c.579dup		p.(Ile194Hisfs*70)	4	4	3.0%	3.2%
c.589C>T		p.(Arg197Cys)	3	3	2.3%	2.4%
c.637C>T		p.(Arg213Trp)	3	3	2.3%	2.4%
c.78G>C		p.(Glu26Asp)	3	3	2.3%	2.4%
Novel Variants						
c.20del		p.Gly7Alafs*119	1	1	0.8%	0.8%
c.185-1G>A		p.(=)	1	1	0.8%	0.8%
c.336_337delinsTT		p.Trp112_Leu113delinsCysPhe	1	1	0.8%	0.8%
c.378del		p.Leu127*	2	2	1.5%	1.6%
c.435dup		p.Ile146AsnfsTer15	1	1	0.8%	0.8%
c.515del		p.Asn172Thrfs*65	1	1	0.8%	0.8%
c.574_580delinsACCCCCCT		p.Pro192Thrfs*72	1	1	0.8%	0.8%

* Sequence variant nomenclature was obtained according to the guidelines of the Human Genome Variation Society (HGVS) by using Mutalyzer (<https://mutalyzer.nl/>).

† In three patients from three different families the variant c.35T>A was in cis with the variant c.52+5G>C, p=.

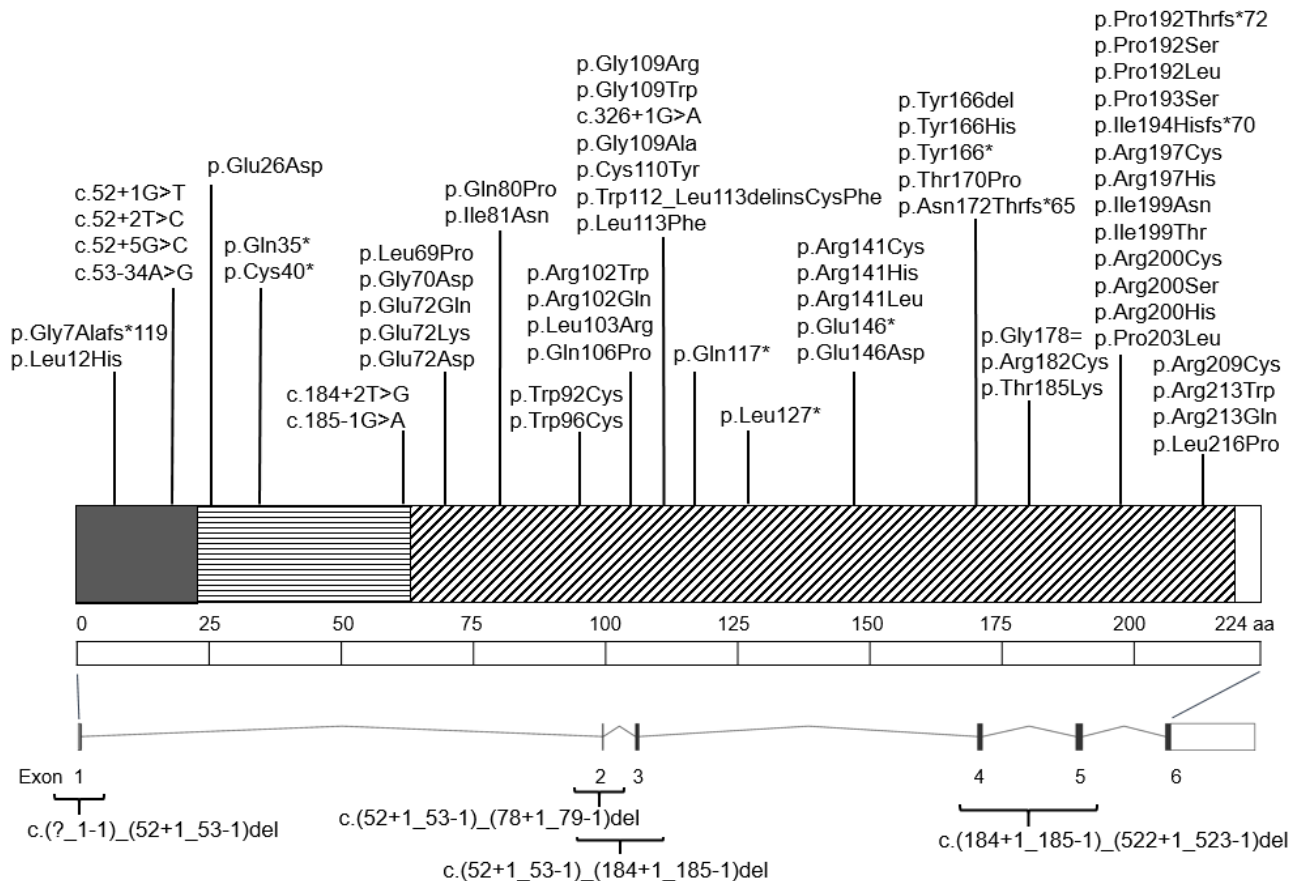


Figure 2: Graphical representation of RS1 gene.

RS1 consist of a signal peptide (amino acids (AA): 1-23, marked with grey), an Rs1 domain (AA: 23-62, marked with horizontal lines) and a discoidin domain (AA: 63-219, marked with diagonal lines). The identified variants in the current cohort are shown in the figure.

Disease Onset

Age of onset was recorded in years for 61 patients. The mean (\pm SD, range, median) age of onset was 16.5 years old (\pm 15.4, 0-58, 11 years). One patient (1.3%) was symptomatic at birth. Half of the patients were symptomatic before the age of 11. Age at baseline examination is detailed in the BCVA section. **Table 2** summarizes

the age of onset and the rest of the clinical findings. **Figure 3** presents the age of onset by age group for the cohort.

Table 2: Clinical Findings

Parameter	Mean \pm SD, range, median
Age of Disease Onset (n=61)	16.5 \pm 15.4, 0-58, 11 years
Common Symptoms and Findings at Presentation (n=75)	
	n= , %
Reduced BCVA	75 (100%)
Nyctalopia	6 (8.5%)
Strabismus	6 (8.5%)
Vitreous Haemorrhage	3 (4.3%)
Retinal Detachment	2 (2.7%)
Nystagmus	1 (1.4%)
Fundoscopy Findings (n=108)	
Bilateral Findings	104 (96.3%)
Unilateral Findings	4 (3.7%)
Macular Schisis	89 (82.4%)
Peripheral Schisis	42 (38.9%)
Macular Atrophy	12 (11.1%)
No findings	4 (3.7%)

BCVA; best corrected visual acuity

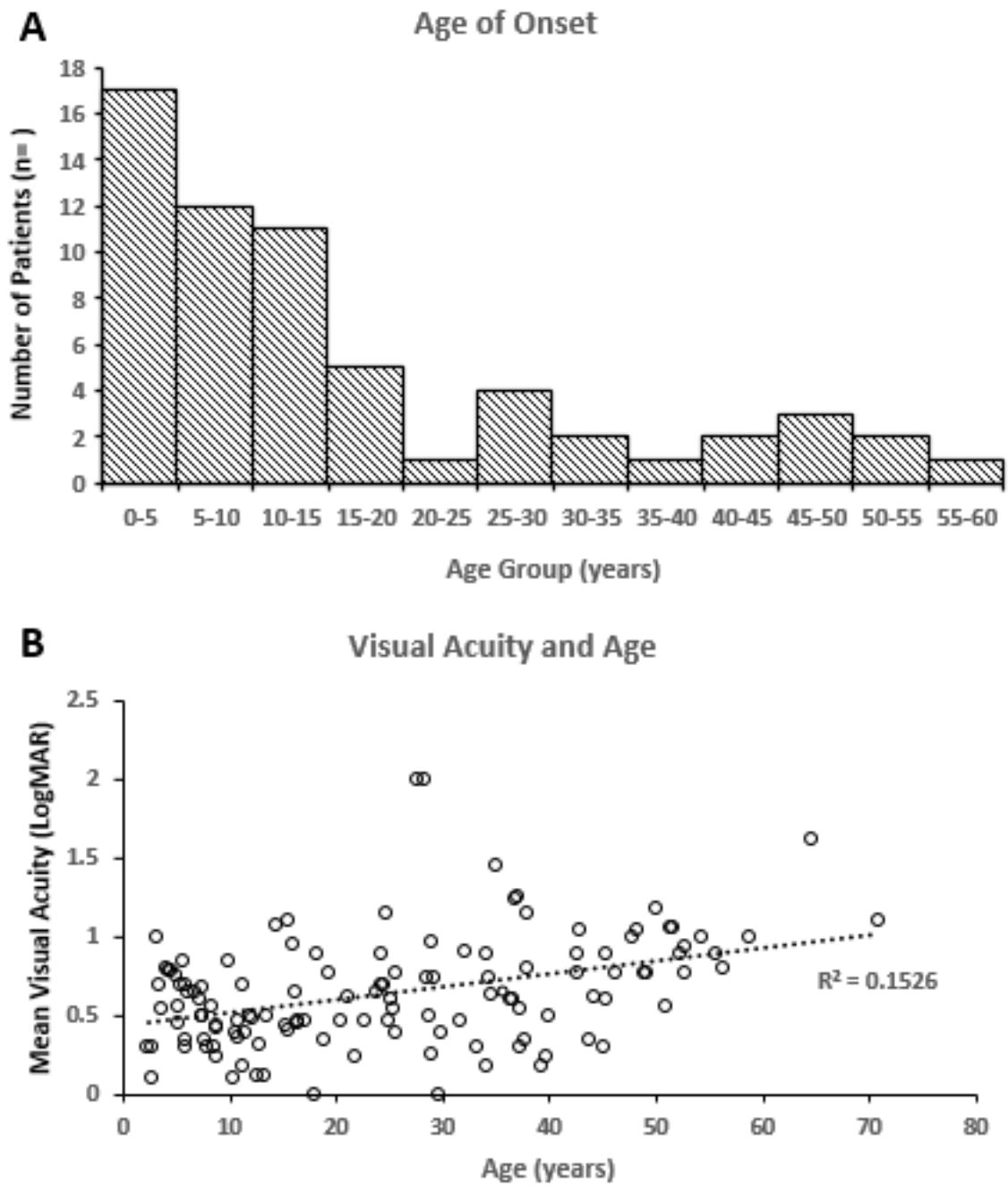


Figure 3.

A. Age of onset by age group; **B.** Mean BCVA against age for the cohort. The moderate correlation can reflect the early severe decrease in BCVA and a further significant slow decline with age.

Signs and Symptoms

Signs and symptoms were available for 75 subjects. Seventy-one patients (94.7%) were symptomatic at presentation. Four patients were asymptomatic at the first evaluation, and were referred for evaluation due to family history of the disease. A universal finding was decreased BCVA (100%). The clinical presentation varied (**Table 2**) but symptoms included nyctalopia (n=6, 8.5%), strabismus (n=6, 8.5%), vitreous hemorrhage (n=3, 4.3%, bilateral in 1 case), retinal detachment (n=2, 2.7%) and nystagmus (n=1, 1.4%). No patient presented with photophobia or reduced color vision.

Fundoscopy findings were documented for 108 patients. Four patient had normal appearing fundi. Findings were bilateral in 104 patients (96.3%) and unilateral in the rest. The most common finding was macular schisis (89 patients, 82.4%), whereas peripheral retinoschisis was present in 42 patients (38.9%). Atrophic macular thinning was present in 12 patients (11.1%). Only one patient had signs of macular atrophy and schisis. The mean age (range) of the patients with macular atrophy was 46.5 years (19-66 years). In contrast, the patients with foveal schisis were younger (mean, range: 22.1, 3-56 years). Fifteen (13.9%) patient developed complications, such as VH and/or RD: 3 patients had VH (2.7%), 6 patients had VH and RD (5.6%), and 6 patients had RD without VH (5.6%).

Visual Acuity

BCVA was assessed cross-sectionally and longitudinally. One hundred and twenty-seven patients had BCVA available at one or more visits. None of the patients had any other vision limiting disease. The mean (\pm SD, range) age at baseline was 25.4 years (\pm 16.7, 2.3 to 70.8 years). Their mean BCVA (\pm SD, range) was 0.65 LogMAR

(± 0.43 , -0.1 to 3.0 LogMAR) for the right eye and 0.64 LogMAR (± 0.44 , 0.0 to 3.0 LogMAR) for the left eye at baseline. Baseline visual acuity was highly variable among subjects, but there was no significant interocular difference ($z=0.27$, $p=0.79$, Wilcoxon Sign Rank test). There was a moderate statistically significant correlation between the mean BCVA for right and left eyes, and the baseline age ($R_2=0.39$, $P<0.00$, Spearman's correlation coefficient). **Figure 3** presents the mean BCVA against age for the cohort. The moderate correlation can reflect the early severe decrease in BCVA and a further significant slow decline with age.

One hundred and thirteen patient had available longitudinal BCVA data. Mean (\pm SD, range) follow-up time was 6.7 years (± 5.2 , 0.2-19.6 years). The mean BCVA (\pm SD, range) was 0.69 LogMAR (± 0.56 , -0.10 to 3.0 LogMAR) and 0.65 LogMAR (± 0.48 , 0.0 to 3.0 LogMAR) for the right and left eyes respectively at the last follow-up. The mean change over follow-up was 0.04 and 0.01 LogMAR for right and left eyes respectively, without significant interocular difference ($p=0.38$, $z=0.88$, Wilcoxon Sign Rank test). There was no significant correlation between the mean rate of BCVA change for right and left eyes, and the baseline age ($R_2=0.15$, $P=0.12$, Spearman's correlation coefficient).

Fundus Autofluorescence

A fundus autofluorescence imaging was available for 108 patients for cross-sectional assessment. Ten patient had low quality imaging in the one eye and two patients for both eyes, that excluded any analysis. In the remaining 96 patients FAF pattern was similar bilaterally. For cross-sectional assessment one eye was included from each patient (106 eyes from 106 patients).

The analysis demonstrated normal results in 16 of 106 eyes (15.09%); 45 eyes (42.45%) showed a spoke-wheel pattern of autofluorescence, 13 eyes (12.26%) showed foveal hyperautofluorescence (“increased central signal” pattern) while 18 eyes (16.98%) showed a “central reduction in signal” pattern. A pattern of central hypoautofluorescence surrounded by hyperautofluorescent borders (“ring of increased signal”) was found in 14 eyes (13.2%): it was isolated in 7 eyes (6.60%) while it was associated with spoke wheel in 3 eyes (2.83%) and with central reduction in signal in 4 eyes (3.77%). **(Table 3)**

Table 3: FAF Findings

Fundus AutoFluorescence Findings (n=106)	n= , %
Normal	16 (15.09%)
Spoke-wheel	45 (42.45%)
Increased central signal	13 (12.26%)
Central reduction in signal	18 (16.98%)
Ring of increased signal	14 (13.21%)

FAF; Fundus AutoFluorescence

A progression from normal FAF appearance to an “increased central signal” pattern was observed in 2 eyes after a mean follow-up of 3 years, to “central reduction in signal” in 1 eye after 11 years, to “ring of increased signal” in 2 eyes after a mean follow-up of 3.5 ± 0.7 years. A progression from “spoke wheel” pattern

to central reduction in signal pattern was detected in 5 eyes after 6 ± 4.8 years, to “increased central signal” pattern in 1 eye after 6 years, to “ring of increased signal” pattern in 1 eye after 10 years and to normal FAF appearance in 3 eyes after a mean of 3.3 ± 3.2 years of follow-up. A progression from “increased central signal” to normal was observed in 1 eye after 3 years of follow-up and to “spoke wheel” pattern in 1 eye after 5 years of follow-up. No change in pattern was observed in eyes with central reduction of signal (as expected).

Optical Coherence Tomography

Spectral domain OCT data were available for 215 eyes of 115 patients at baseline. A foveoschisis was observed in 172 of 215 eyes (80%), a parafoveal schisis was present in 171 of 215 eyes (79.5%), and foveal atrophy was observed in 44 of 215 eyes (20.47%). The localization of the cystoid changes was mapped for 181 eyes at baseline: cysts were localized mainly in the inner nuclear layer (172/181 eyes [95%]), in the outer nuclear layer (97/181 eyes [53.6%]) and in the ganglion cell layer (92/181 eyes [50.83%]). Cysts were observed in the outer plexiform layer in 41/181 eyes (22.65%), and in the inner plexiform layer in only 1 of 181 eyes (0.55%). Retinal nerve fiber layer was involved by cysts in 2/181 eyes (1.1%). The mean central macular thickness was $378.15 \pm 162.13 \mu\text{m}$ (range, 46-1099 μm). Qualitative analysis of photoreceptor structure has been performed at baseline and the most frequently affected structure was the IZ which was analysed in 220 eyes at baseline and found to be disrupted in 139 eyes (63.18%) and continuous in 81 eyes (36.82%). The EZ analysis was possible in 218 eyes: it was disrupted in 133 eyes (61%) and continuous in 85 eyes (39%). Mean PROS length was available for 66 patients with a mean age of 27.7 ± 17.5 years at baseline and it measured $36.85 \pm 7.26 \mu\text{m}$ (range, 15-56 μm). **(Table 4)**

Follow-up OCT imaging was available for 187 eyes of 115 patients and the results were elaborated as follow. **(Table 5)**

Table 4: OCT findings at baseline

Parameter	n= , %
Foveoschisis	172/215 (80%)
Parafoveal schisis	171/215 (79.5%)
Foveal atrophy	44/215 (20.47%)
Cyst Localization (n = 181)	n= , %
RNFL	2/181 (1.1%)
GCL	92/181 (50.83%)
IPL	1/181 (0.55%)
INL	172/181 (95%)
OPL	41/181 (22.65%)
ONL	97/181 (53.6%)
CMT μm	
Mean \pm SD	378.15 \pm 162.13
Range	46-1099 μm
PROS length μm	
Mean \pm SD	36.85 \pm 7.26
Range	15-56
Outer retinal defects	n= , %
Ellipsoid zone	133 (61%)
Interdigitation zone	139 (63.18%)

CMT = central macular thickness; GCL = ganglion cell layer; IPL= inner plexiform layer; IPL = inner plexiform layer; INL = inner nuclear layer; OPL = outer plexiform layer; ONL = outer nuclear layer, PROS = photoreceptor outer segment; RNFL = retinal nerve fiber layer; SD = standard deviation.

Table 5: OCT findings at follow-up

Parameter	n= , %
Foveoschisis	140/187 (74.86%)
Parafoveal schisis	129/187 (68.9%)
Foveal atrophy	41/187 (21.93%)
Cyst Localization (n = 175)	n= , %
RNFL	0/175 (0%)
GCL	85/175 (48.57%)
IPL	0/181 (0%)
INL	164/175 (93.71%)
OPL	34/175 (19.43%)
ONL	96/175 (54.86%)
CMT μm	
Mean \pm SD	348.87 \pm 164.15
Range	28-1130 μm
PROS length μm	
Mean \pm SD	30.5 \pm 6.89
Range	22-53
Outer retinal defects	n= , %
Ellipsoid zone	118 (64.13%)
Interdigitation zone	119 (65%)

CMT = central macular thickness; GCL = ganglion cell layer; IPL= inner plexiform layer; IPL = inner plexiform layer; INL = inner nuclear layer; OPL = outer plexiform layer; ONL = outer nuclear layer, PROS = photoreceptor outer segment; RNFL = retinal nerve fiber layer; SD = standard deviation.

A foveoschisis was observed in 140 of 187 eyes (74.86%), a parafoveal schisis was present in 129 of 187 eyes (68.9%) and foveal atrophy was observed in 41 of 187 eyes (21.93%). Data on cystoid changes were available for 175 eyes: cysts were localized mainly in the inner nuclear layer (164 eyes/175 [93.71%]), in the outer nuclear layer (96/175 eyes [54.86%]) and in the ganglion cell layer (85/175 [48.57%]). Cysts were observed in the outer plexiform layer in 34/175 eyes

(19.43%). The mean central macular thickness was $348.87 \pm 164.15 \mu\text{m}$ (range, 28-1130 μm). No cysts were detected in the inner plexiform layer and in the retinal nerve fiber layer.

Qualitative analysis of photoreceptor structure has been performed at the last follow-up and the most frequently affected structure was the IZ which was analyzed in 183 eyes at baseline and found to be disrupted in 119 eyes (65%) and continuous in 64 eyes (35%). The EZ analysis was possible in 184 eyes: it was disrupted in 118 eyes (64.13%) and continuous in 66 eyes (55.46%). Mean PROS length was available for 119 patients with a mean age of 30.5 ± 17.3 years at the last follow-up and it measured $36.38 \pm 6.89 \mu\text{m}$ (range, 22-53 μm).

3.1 CASE REPORTS

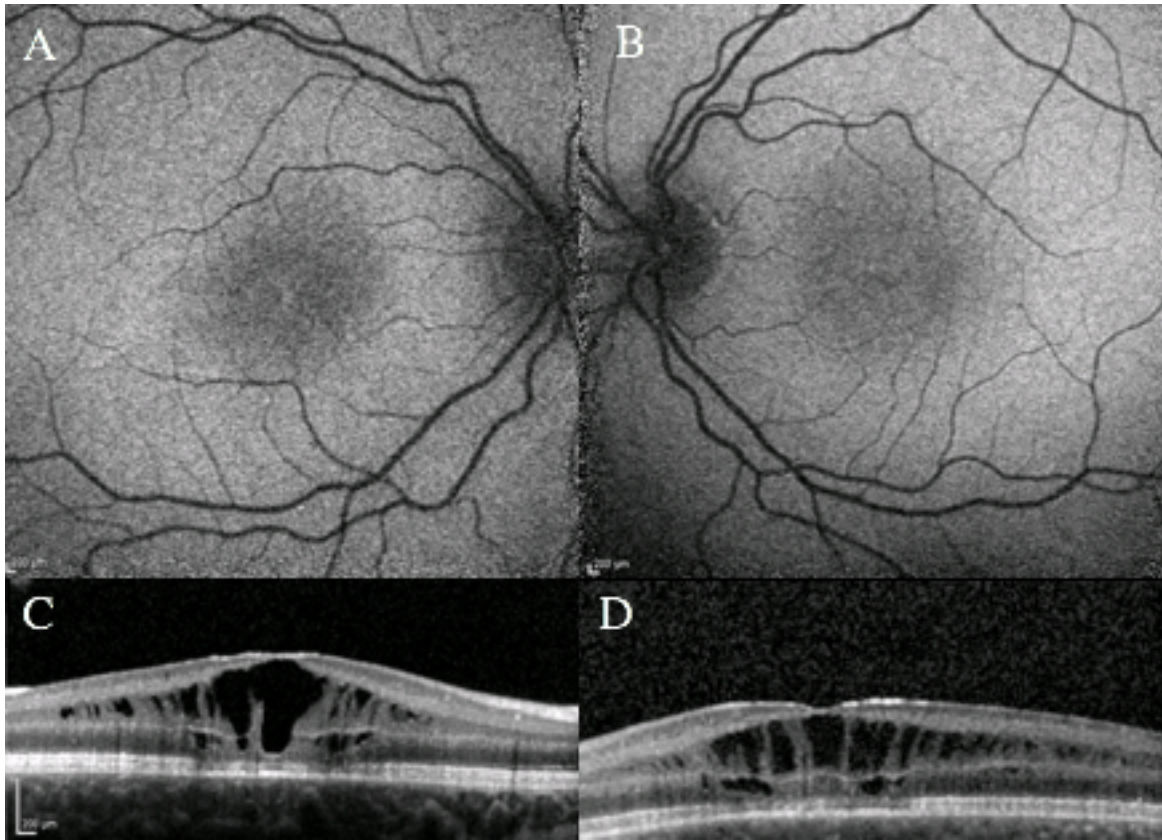


Figure 4. Case report MEH 030, 6 year-old boy with X-linked retinoschisis. The visual acuity is 0.16 LogMAR in the right eye and 0.42 LogMAR in the left eye. A and B: Spectralis Fundus AutoFluorescence (FAF) of the right eye and left eye respectively. C and D: OCT of the right eye and left eye respectively, at baseline.

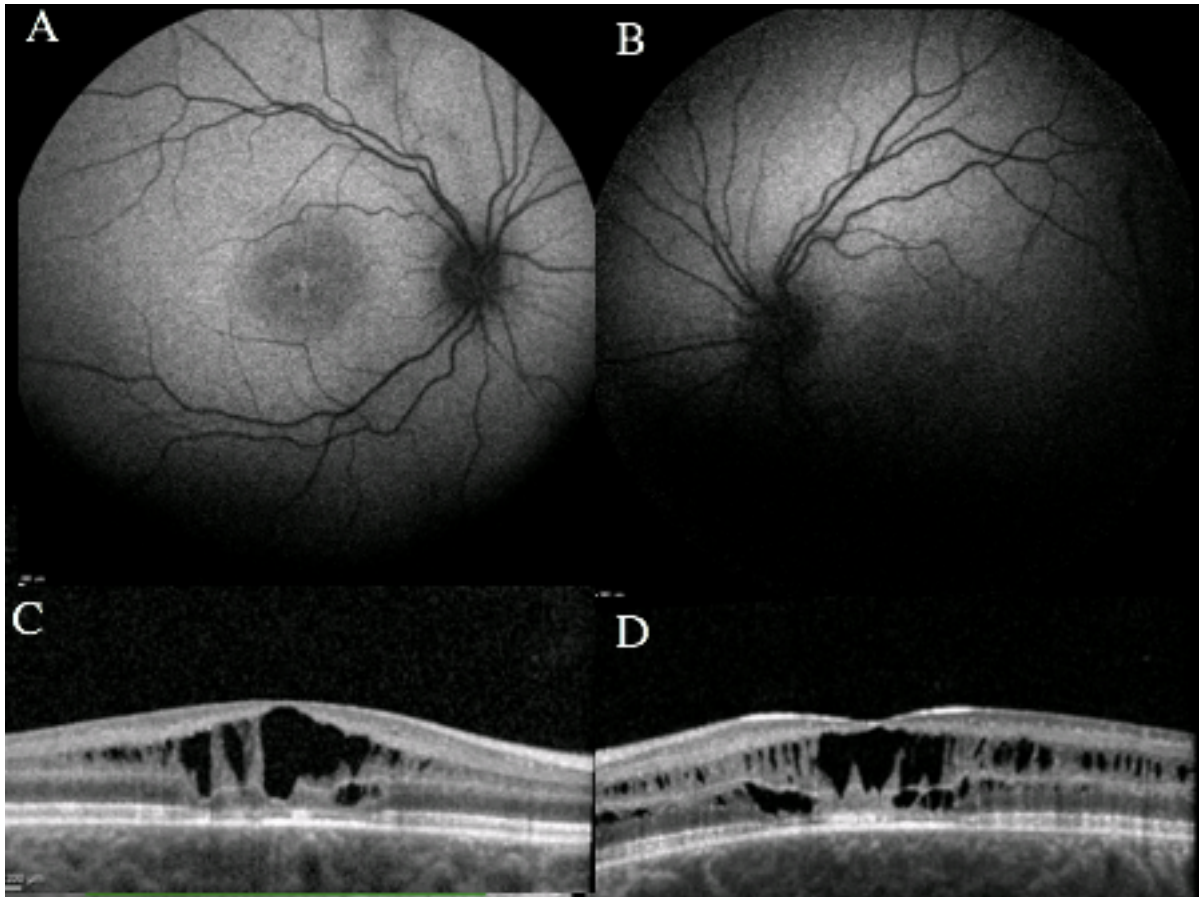


Figure 5. Case report MEH 030, (previous case), 10 year-old boy with X-linked retinoschisis at 4 years follow-up. The visual acuity is 0 LogMAR in the right eye and 0.17 LogMAR in the left eye (a therapy for amblyopia in the LE has been performed). A and B: Spectralis FAF of the right eye and left eye respectively. C and D: OCT of the right eye and left eye respectively. The imaging shows stability of the disease over 4 years of follow-up.

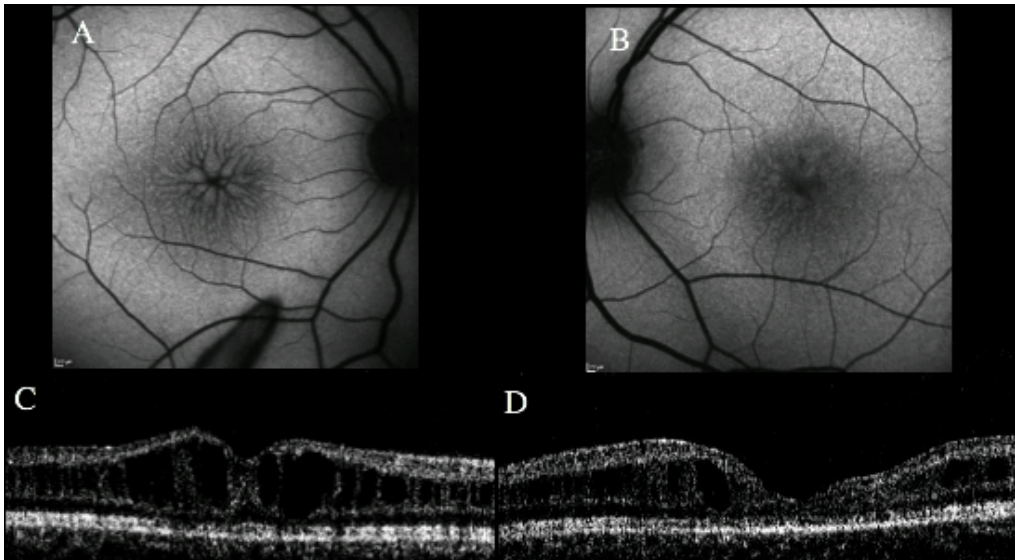


Figure 6. MEH 057, 25 year old male with X-linked Retinoschisis. A, B: Spectralis FAF. C and D: Topcon OCT.

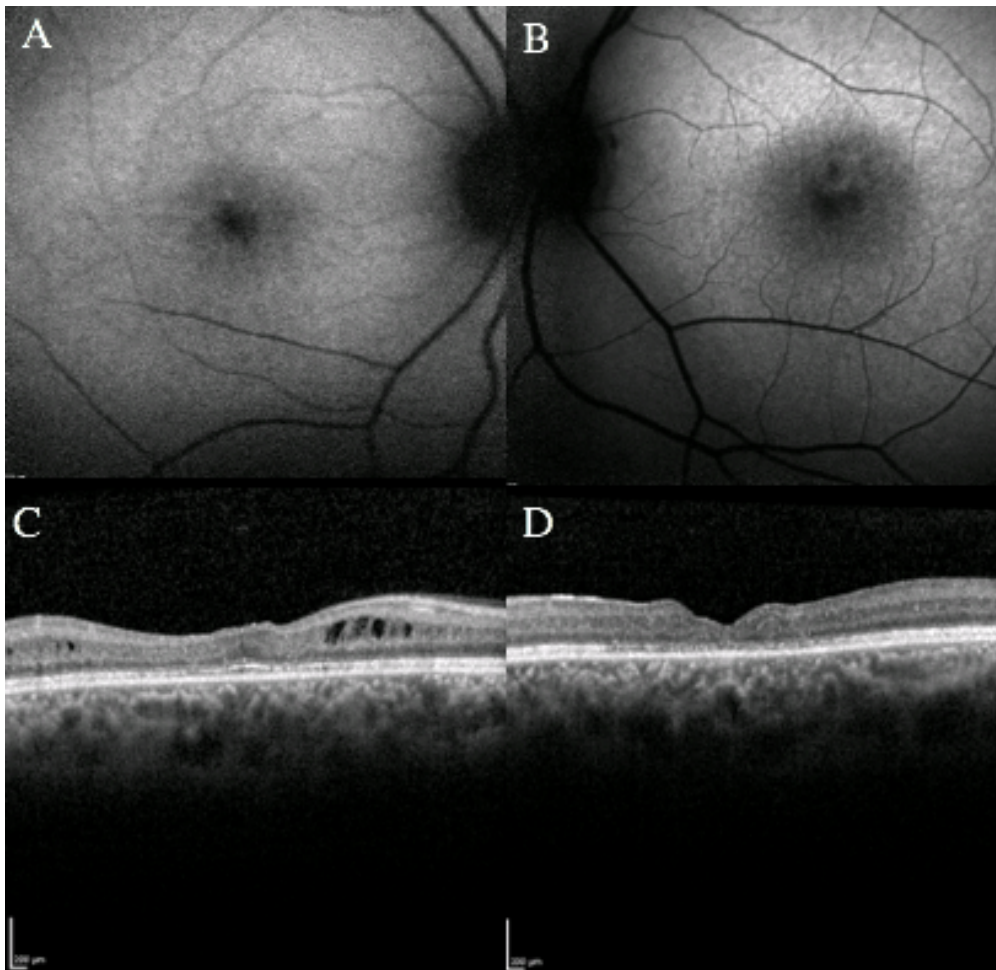


Figure 7. MEH057 (previous case), 31 years-old male with X-linked Retinoschisis after 6 years follow-up from baseline (Figure 6). A, B: Spectralis FAF. C and D: Spectralis OCT. A progression to macular atrophy can be seen. The visual acuity

is 0.77 LogMar in the Right eye and 0.77 LogMar in the Left eye after therapy with acetazolamide.

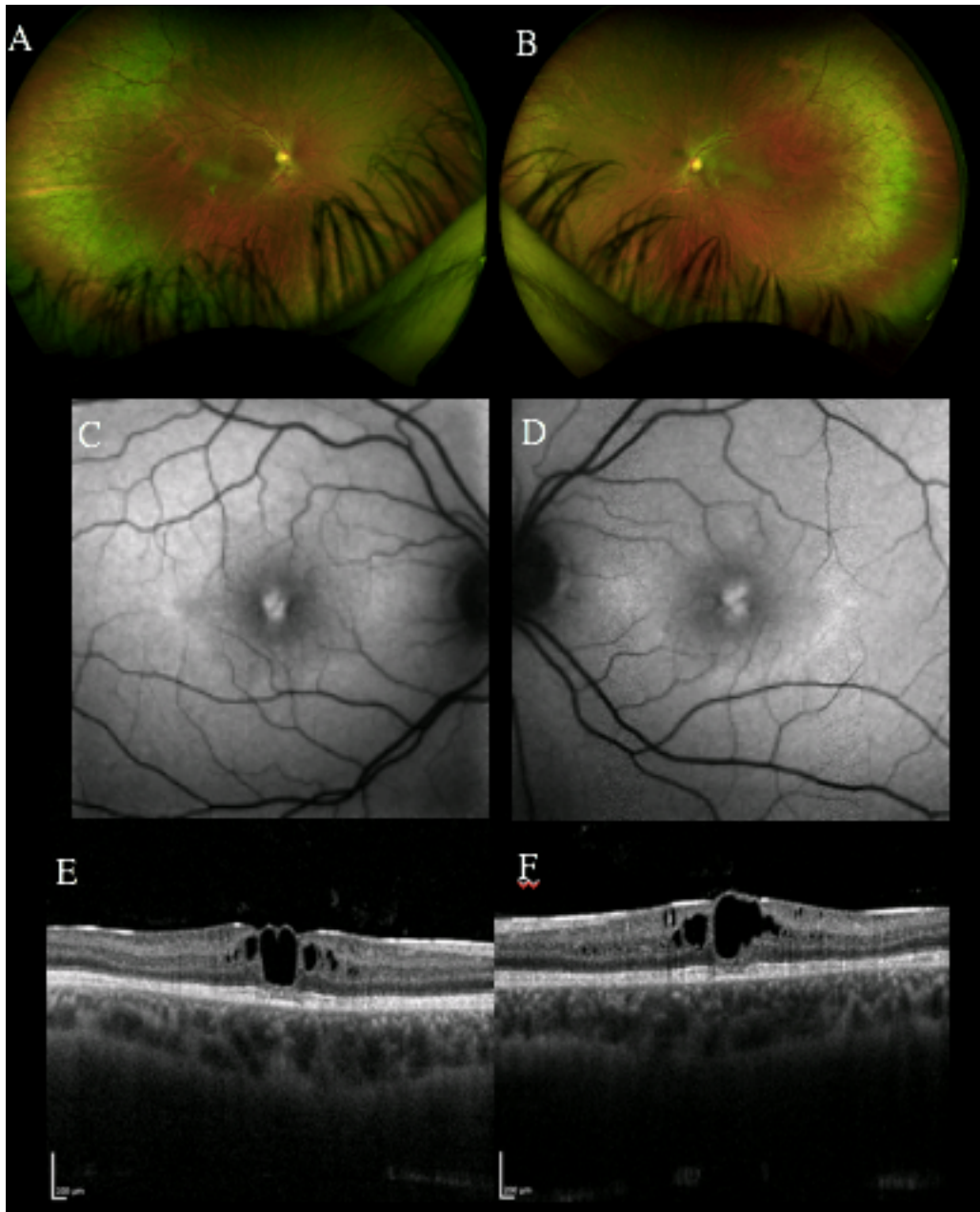


Figure 8. Case report MEH 048, 23 year-old male with X-linked retinoschisis. The visual acuity is 0.17 LogMAR in the right eye and 0.17 LogMAR in the left eye. A and B: Pseudocolour Optos fundus photograph, C and D: Spectralis FAF of the right eye and left eye respectively. E and F: Spectralis OCT of the right eye and left eye respectively. The retina imaging shows symmetry of the disease.

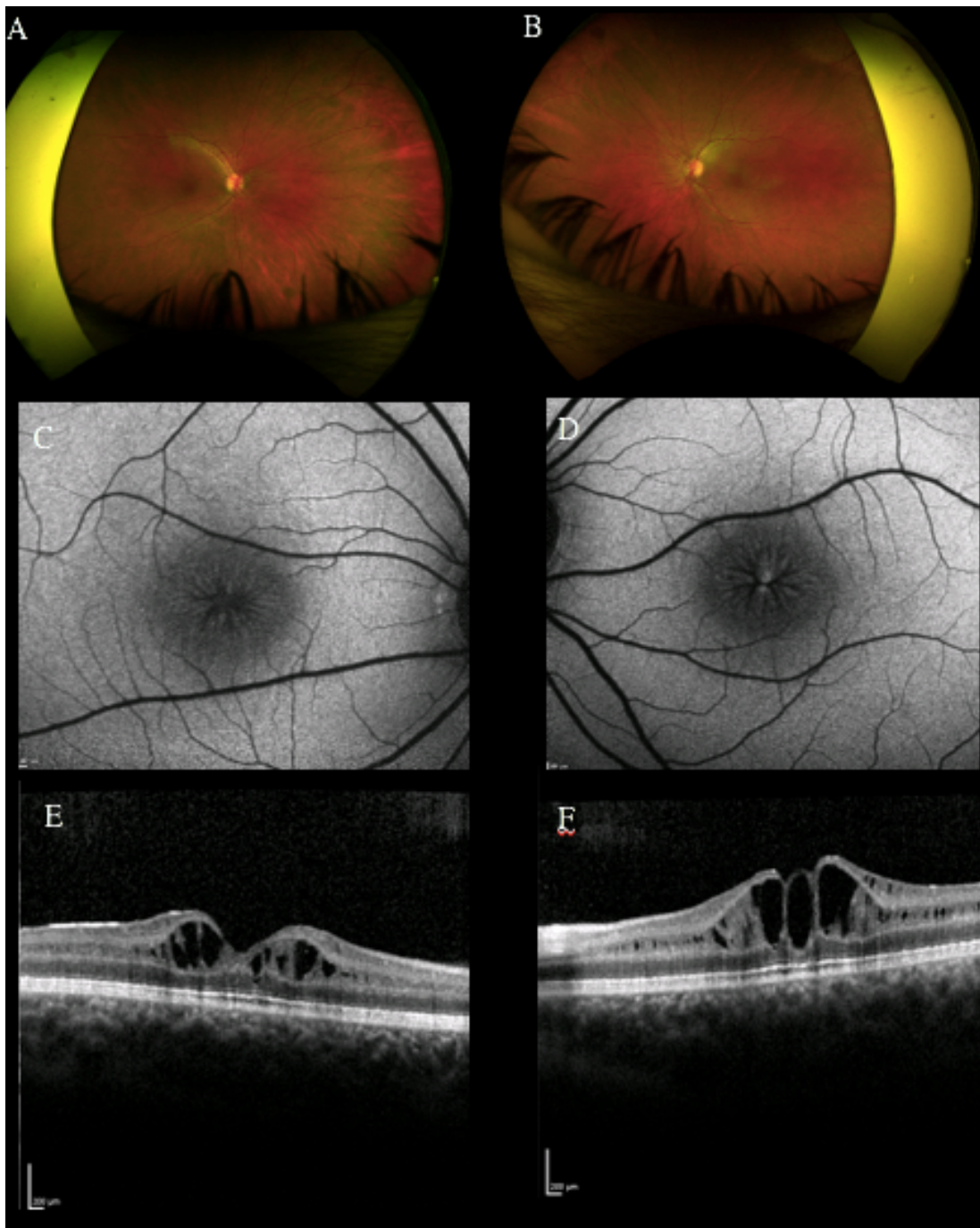


Figure 9. Case report MEH 029, 17 year-old male with X linked retinoschisis. The visual acuity is 0.30 LogMAR in the right eye and 0.60 LogMAR in the left eye. A and B: Pseudocolour Optos fundus photograph, C and D: Spectralis FAF of the right eye and left eye respectively. E and F: Spectralis OCT of the right eye and left eye respectively. The fundus autofluorescence shows a typical “spoke wheel” pattern.

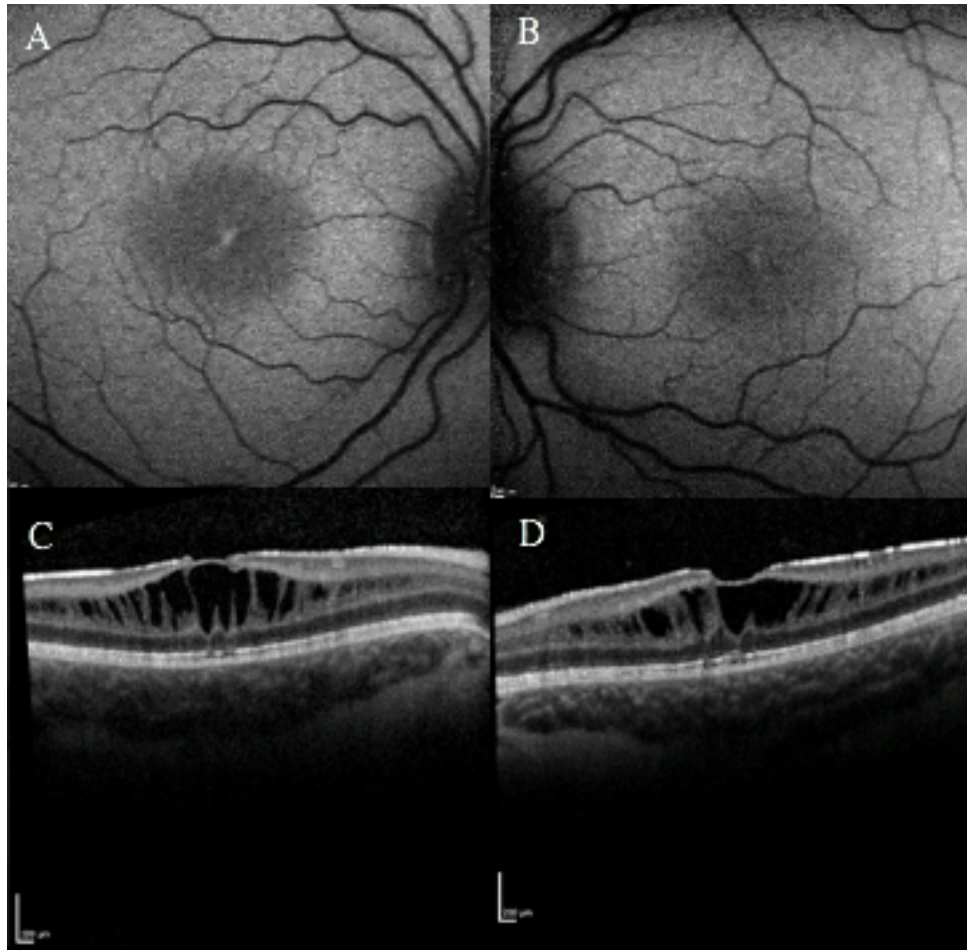


Figure 10. Case report MEH 016, 8 year-old boy with X-linked retinoschisis. The visual acuity is 0.38 LogMAR in the right eye and 0.30 LogMAR in the left eye. A and B: Spectralis FAF of the right eye and left eye respectively. C and D: Spectralis OCT of the right eye and left eye respectively. The fundus autofluorescence shows an “increased signal” pattern.

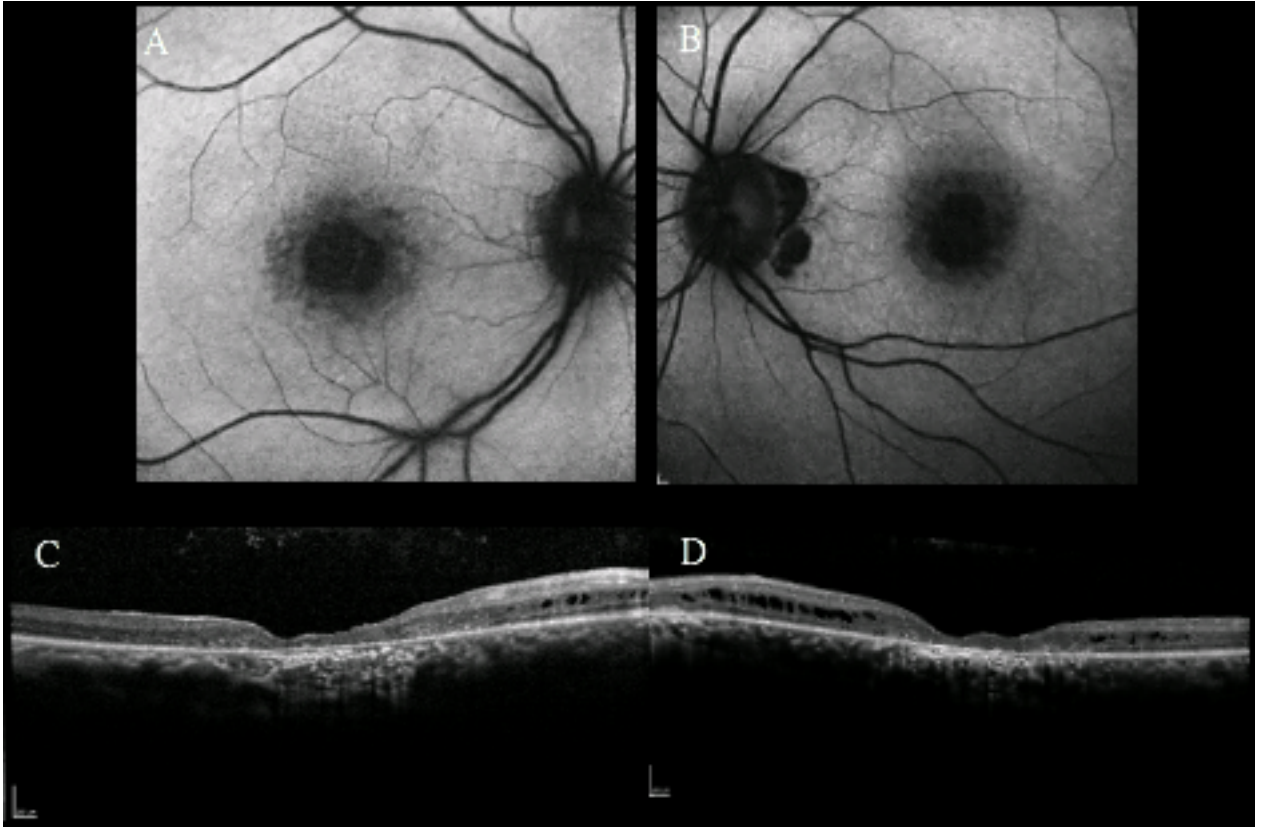


Figure 11. Case report MEH 039, 44 year-old male with X-linked retinoschisis. The visual acuity is 1.30 LogMAR in the right eye and 1 LogMAR in the left eye. A and B: Spectralis FAF of the right eye and left eye respectively. C and D: Spectralis OCT of the right eye and left eye respectively. The fundus autofluorescence shows a “central reduction in signal” pattern.

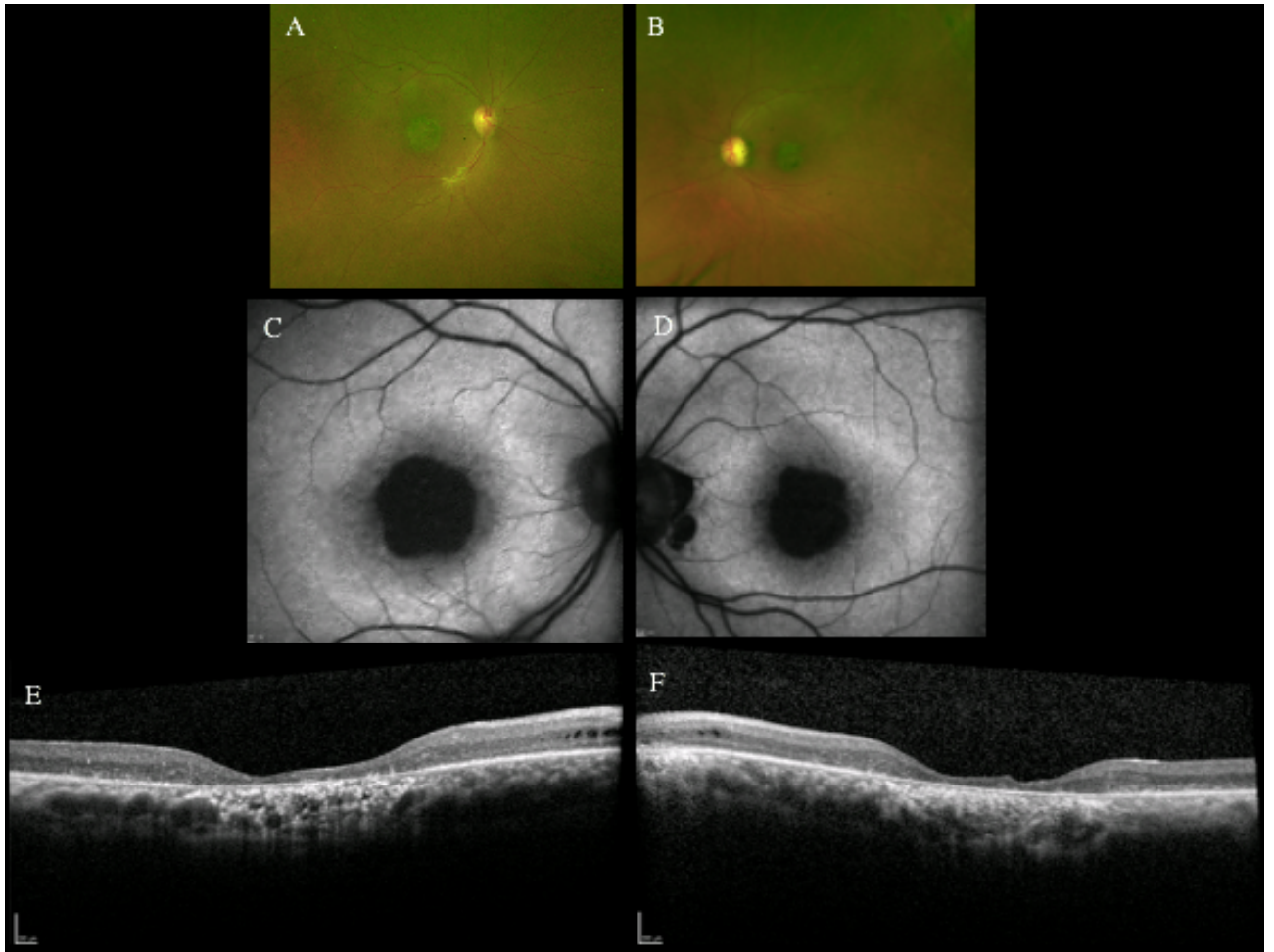


Figure 12. Case report MEH 039 (previous case), 51 year-old male with X-linked retinoschisis. The visual acuity is 1.77 LogMAR in the right eye and 1 LogMAR in the left eye. A and B: Pseudocolour Optos fundus photograph; C and D: Spectralis FAF; E and F: Spectralis OCT of the right eye and left eye respectively. The fundus autofluorescence shows a progression of the “central reduction in signal” pattern (atrophy) during the 7 years follow-up.

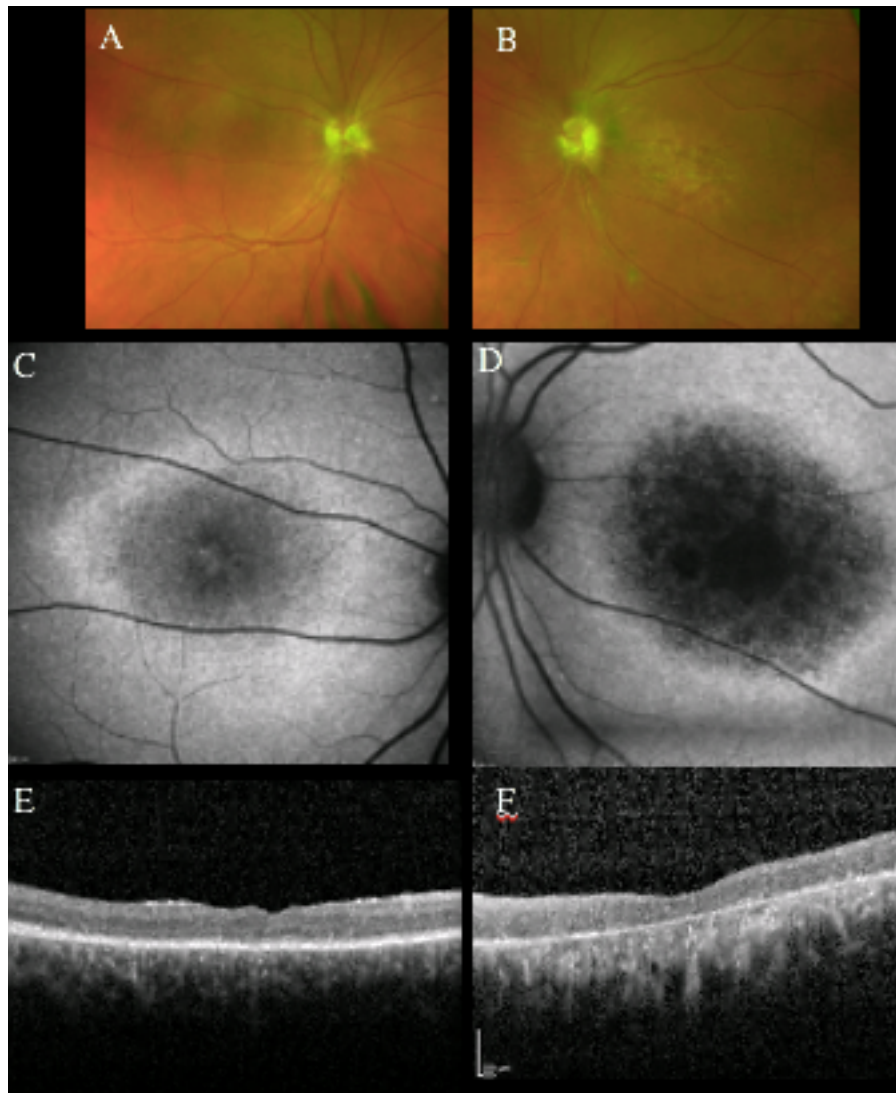


Figure 13. Case report MEH 038, 34 year-old male with X-linked retinoschisis. The visual acuity is 0.77 LogMAR in the right eye and 1.30 LogMAR in the left eye. A and B: Pseudocolour Optos fundus photograph; C and D: Spectralis FAF; E and F: Spectralis OCT of the right eye and left eye respectively. The fundus autofluorescence shows a “ring of increased signal” pattern.

4. DISCUSSION

The current study describes the genetic and clinical characteristics of 132 males from 126 families with molecularly confirmed XLRS. It represents the largest cohort to date to undergo clinical and genetic analysis. Our results provide an outline of the retinal phenotype and disease natural history for XLRS, over a wide range of age.

Over 200 disease-causing mutations in the RS1 gene are known with most mutations occurring as non-synonymous changes in the major protein unit (discoidin domain, **Figure 2**). In our study in total 66 variants were identified of which seven were novel. We found that missense variants were the most common type of alteration (72.7%) in agreement with Gao et al. 2020. Previous publications have pointed to the spectrum of disease phenotype observed across individuals with XLRS. In those studies, a variety of factors were thought to contribute to the spectrum of clinical manifestation observed, including underlying mutation (Bowles et al. IOVS 2011) and mainly age. (Bowles et al 2011, Menke et al. 2011, Lesch et al.2008, Apushkin et al. 2005) Human studies have shown that there is a wide heterogeneity with variable fundus appearance in patients with various mutations, and also within families with the same mutation, and no correlation has been identified between mutation type and disease severity or progression. (Eksandh et al. 2000, Pimenides et al. 2005, Simonelli et al. 2003). The patients in our cohort showed profound phenotypic variability and we did not find any clear genotype or phenotype correlation.

The most common retinal finding was macular schisis (89 patients, 82.4%), whereas peripheral retinoschisis was present in more than one third of the patients (n=42, 38.9%). Atrophic macular thinning was present in 12 patients (11.1%). Only one patient had signs of macular atrophy and schisis. The clinical characteristics of

the subjects were generally similar to those in other published studies (Apushkin et al. 2005, George et al. 1996). They reported macular schisis from 68% to 100% of patients (Fahim 2017), peripheral retinoschisis in 43% to 60% of subjects (George 1996) and retinal atrophy in 8% to 10% of patients. Some studies reported atrophic macular thinning in patients in their fourth decade of life and clinical descriptions of macular schisis flattening with age without clear mechanism for these changes. (Menke et al. 2011, Genead et al. 2010) In our study we found that the mean age (range) of the patients with macular atrophy was 46.5 years (19-66 years). In contrast, the patients with foveal schisis were younger (mean, range: 22.1, 3-56 years). We can hypothesize that the natural history of the disease presents a normal fundus in younger patients then the retinoschisis develops and finally a macular atrophy slowly appears at an older age, defining the late stage of the disease.

Fifteen (13,9%) patients developed complications, such as VH and/or RD: 3 patients had VH (2.7%), 6 patients had VH and RD (5.6%), and 6 patients had RD without VH (5.6%). Frequency of complications, such as vitreous haemorrhage and retinal detachment reported here is similar compared to that reported by some authors who found a frequency between 3% to 21% for vitreous haemorrhage and 5% to 40% for retinal detachment. (George 1996, Kellner 1990, Roesch 1998, Fahim 2017)

The mean BCVA (\pm SD, range) was 0.65 LogMAR (\pm 0.43, -0.1 to 3.0 LogMAR) for the right eye and 0.64 LogMAR (\pm 0.44, 0.0 to 3.0 LogMAR) for the left eye at baseline. The mean BCVA (\pm SD, range) was 0.69 LogMAR (\pm 0.56, -0.10 to 3.0 LogMAR) and 0.65 LogMAR (\pm 0.48, 0.0 to 3.0 LogMAR) for the right and left eyes respectively at the last follow-up. The mean change over follow-up was 0.04 and 0.01 LogMAR for right and left eyes respectively, without significant interocular

difference. Orès et al. found a mean BCVA of 0.6 ± 0.38 LogMar and Gao et al. reported a mean BCVA of 0.28 ± 0.17 (range 20/1000-20/25) Our data indicate an overall stability of the disease. There was a moderate statistically significant correlation between the mean BCVA for right and left eyes, and the baseline age. The moderate correlation can reflect the early severe decrease in BCVA and a further significant slow decline with age.

FAF results seemed to be highly variable: the analysis demonstrated normal results in 16 of 106 eyes (15.09%); 45 eyes (42.45%) showed a spoke-wheel pattern of autofluorescence, 13 eyes (12.26%) showed foveal hyperautofluorescence (“increased central signal” pattern) while 18 eyes (16.98%) showed a “central reduction in signal” pattern. A pattern of central hypoautofluorescence surrounded by hyperautofluorescent borders (“ring of increase signal”) was found in 14 eyes (13.2%): it was isolated in 7 eyes (6.60%) while it was associated with spoke wheel in 3 eyes (2.83%) and with central reduction in signal in 4 eyes (3.77%). This variability in FAF appearance has been reported before (Renner et al. 2008, Vincent et al. 2013). De Silva et al reported that the spoke-wheel pattern of high and low intensity signal represents the characteristic autofluorescent finding in patient with XLR5 and it is due to displacement of luteal pigment. (De Silva et al. 2020). Nevertheless we reported that it has been only identified in approximately half of patients in agreement with previous studies. (Orès et al. 2018, Vincent et al. 2013) Over time, FAF can document progression in terms of RPE changes. We can speculate that there is a progression from an “increase central signal” pattern, to “spoke wheel” pattern, throughout an increased “ring of increase signal” to a final pattern of “central reduction in signal”.

Spectral domain OCT data were available for 215 eyes of 115 patients at baseline and they showed that foveoschisis was observed in 172 of 215 eyes (80%), a parafoveal schisis was present in 171 of 215 eyes (79.5%), and foveal atrophy was observed in 44 of 215 eyes (20.47%) which is similar to earlier findings who found foveal and parafoveal foveoschisis in most cases (88%) and macular atrophy observed in older patients (11%). (Orès et al. 2018 and Gao et al. 2020) In our study at the last follow-up a foveoschisis was observed in 140 of 187 eyes (74.86%), a parafoveal schisis was present in 129 of 187 eyes (68.9%) and foveal atrophy was observed in 41 of 187 eyes (21.93%). The mechanism that leads to the occurrence of different types of schisis is not well understood.

Studies show that the schisis can involve different layers of retina, supporting the idea of a phenotypical variability. Some authors demonstrated that foveal schisis occurs mostly in the INL and OPL/ONL. (Eriksson et al. 2004, Gregori et al. 2009, Yu J et al. 2010, Andreoli et al. Am J O 2014) Moreover inner nuclear layer was found to be the most common site of schisis. (Padròn-Pérez et al. 2018) We found that the main manifestation of schisis at baseline were at the INL (95%), ONL (53.6%) and OPL (22.65%). GCL was affected in 50.83% of eyes. Our finding parallel those reported by Andreoli et al (Andreoli et al. 2014) who found that schisis affected the INL and OPL, respectively, in 85% and 61% of cases and Orès et al (Orès et al 2018) who identified schisis changes mainly in the INL (88%) and OPL (64%), followed by RNFL/GCL(46%) and ONL (22%). In almost half of the eyes, cysts also were found in GCL, in accordance with the previous reports (Gregori et al. 2009, Yu et al. 2010, Yang et al. 2014)

In our study we found at the last follow-up that cysts were localized mainly in the inner nuclear layer (164 eyes/175 [93.71%]), in the outer nuclear layer (96 of 175

eyes [54.86%]) and in the ganglion cell layer (85/175 [48.57%]). Cysts were observed in the outer plexiform layer in 34 eyes/175 (19.43%). No cysts were detected in the inner plexiform layer and in the retinal nerve fiber layer. These data indicate that retinoschisis is widely distributed in the retina and the cysts' distribution may change over time.

Other structural alterations of photoreceptors like thinning, ellipsoid zone defects within the RPE alterations, atrophy as well as normal macular structure (8% of eyes) (Fahim et al 2017) were also noted. We confirm the frequent qualitative defects in outer photoreceptor structure showing a disrupted IZ in 63.18% of eyes at baseline and in 65% at the last follow-up. The EZ was disrupted in 61% at baseline and in 64.13% of eye at the last follow-up. We confirm the results of Orès et al who found that the most frequent defect was the IZ alteration, supporting the hypothesis that the IZ defect may reflect the initial changes in photoreceptors. (Yang et al. 2014, Yu et al. 2010)

The main limitations of our study are the retrospective design, the lack of a control group and the widely variable follow-up of subjects. One additional limitation of this study is that we did not consider ERG examination and therefore we could not compare disease severity with the type of ERG abnormality. Another limitation was the absence of the analysis of the effect of the therapy that might have affected the results at the last follow-up.

In summary, this study provide comprehensive analysis of the genetic and clinical characteristics of the largest XLRS cohort reported in the literature, with a long-term follow up, elucidating disease natural history. XLRS has a wide spectrum of clinical characteristics, hence, molecular diagnosis is crucial for its diagnosis and genetic counselling, as well for patient's participation in gene directed trials. It's

imperative to understand the natural progression of the disease and to perform a precise phenotypic characterization when choosing outcome measures to monitor disease progression and outcomes of therapeutic interventions. XLRS appear to have a wide window of therapeutic intervention, with a most of the patients preserving residual foveal structural till the fourth decade of life.

Supplementary Table 1: *RS1* gene variants

Gene	Nucleotide change	Amino acid change	Position	Coding impact	Location	dbSNP ID
RS1	c.20del	p.Gly7Alafs*119	18690169	frameshift	exon 1 of 6 position 60 of 92 (coding, NMD)	NA
RS1	c.35T>A	p.Leu12His	18690154	missense	exon 1 of 6 position 75 of 92 (coding)	rs62645879
RS1	c.52+1G>T		18690136	splice site alteration	intron 1 of 5 position 1 of 14351 (splicing-ACMG, splicing, intronic)	rs281865336
RS1	c.52+2T>C		18690135	splice site alteration	intron 1 of 5 position 2 of 14351 (splicing-ACMG, splicing, intronic)	rs281865334
RS1	c.52+5G>C		18690132	intron	intron 1 of 5 position 5 of 14351 (splicing, intronic)	rs281865338
RS1	c.53-34A>G		18675819	deep intron	intron 1 of 5 position 14318 of 14351 (intronic)	NA
RS1	c.78G>C	p.Glu26Asp	18675760	missense	exon 2 of 6 position 26 of 26 (splicing-ACMG, splicing, coding)	NA
RS1	c.103C>T	p.Gln35*	18674854	nonsense	exon 3 of 6 position 25 of 106 (coding, NMD)	NA
RS1	c.120C>A	p.Cys40*	18674837	nonsense	exon 3 of 6 position 42 of 106 (coding, NMD)	rs62645885
RS1	c.184+2T>G		18674771	splice site alteration	intron 3 of 5 position 2 of 9320 (splicing-ACMG, splicing, intronic)	rs1555959367
RS1	c.185-1G>A		18665453	splice site alteration	intron 3 of 5 position 9320 of 9320 (splicing-ACMG, splicing, intronic)	rs281865344
RS1	c.206T>C	p.Leu69Pro	18665431	missense	exon 4 of 6 position 22 of 142 (coding)	NA
RS1	c.209G>A	p.Gly70Asp	18665428	missense	exon 4 of 6 position 25 of 142 (coding)	rs62645895
RS1	c.214G>C	p.Glu72Gln	18665423	missense	exon 4 of 6 position 30 of 142 (coding)	rs104894928
RS1	c.214G>A	p.Glu72Lys	18665423	missense	exon 4 of 6 position 30 of 142 (coding)	rs104894928
RS1	c.216G>C	p.Glu72Asp	18665421	missense	exon 4 of 6 position 32 of 142 (coding)	rs104894932
RS1	c.239A>C	p.Gln80Pro	18665398	missense	exon 5 of 6 position 55 of 142 (coding)	NA
RS1	c.242T>A	p.Ile81Asn	18665395	missense	exon 4 of 6 position 58 of 142 (coding)	rs61750457
RS1	c.276G>C	p.Trp92Cys	18665361	missense	exon 4 of 6 position 92 of 142 (coding)	rs61752062
RS1	c.288G>C	p.Trp96Cys	18665349	missense	exon 4 of 6 position 104 of 142 (coding)	NA
RS1	c.304C>T	p.Arg102Trp	18665333	missense	exon 4 of 6 position 120 of 142 (coding)	rs61752067
RS1	c.305G>A	p.Arg102Gln	18665332	missense	exon 4 of 6 position 121 of 142 (coding)	rs61752068
RS1	c.308T>G	p.Leu103Arg	18665329	missense	exon 4 of 6 position 124 of 142 (coding)	rs61752069
RS1	c.317A>C	p.Gln106Pro	18665320	missense	exon 4 of 6 position 133 of 142 (splicing, coding)	NA
RS1	c.325G>C	p.Gly109Arg	18665312	missense	exon 4 of 6 position 141 of 142 (splicing-ACMG, splicing, coding)	rs104894934
RS1	c.325G>T	p.Gly109Trp	18665312	missense	exon 4 of 6 position 141 of 142 (splicing-ACMG, splicing, coding)	rs104894934
RS1	c.326+1G>A		18665310	splice site alteration	intron 4 of 5 position 1 of 2565 (splicing-ACMG, splicing, intronic)	rs281865346
RS1	c.326G>C	p.Gly109Ala	18665311	missense	exon 4 of 6 position 142 of 142 (splicing-ACMG, splicing, coding)	NA
RS1	c.329G>A	p.Cys110Tyr	18662743	missense	exon 5 of 6 position 3 of 196 (splicing, coding)	rs61752075
RS1	c.336_337delinsTT	p.Trp112_Leu113delinsCysPhe	18662735	in frame	exon 5 of 6 position 10-11 of 196 (splicing, coding)	NA
RS1	c.337C>T	p.Leu113Phe	18662735	missense	exon 5 of 6 position 11 of 196 (coding)	rs61752145
RS1	c.349C>G	p.Gln117*	18662723	nonsense	exon 5 of 6 position 23 of 196 (coding, NMD)	rs199469696
RS1	c.378del	p.Leu127*	18662694	nonsense	exon 5 of 6 position 52 of 196 (coding, NMD)	NA
RS1	c.421C>T	p.Arg141Cys	18662651	missense	exon 5 of 6 position 95 of 196 (coding)	rs61752158
RS1	c.422G>A	p.Arg141His	18662650	missense	exon 5 of 6 position 96 of 196 (coding)	rs61752159
RS1	c.422G>T	p.Arg141Leu	18662650	missense	exon 5 of 6 position 96 of 196 (coding)	NA
RS1	c.435dup	p.Ile146AsnfsTer15	18662637	frameshift	exon 4 of 50 before position 135 of 140 (splicing, coding, NMD)	NA
RS1	c.438G>C	p.Glu146Asp	18662634	missense	exon 5 of 6 position 112 of 196 (coding)	rs61753163 dbSNP
RS1	c.496_498del	p.Tyr166del	18662574	in frame	exon 5 of 6 position 170-172 of 196 (coding)	NA
RS1	c.496T>C	p.Tyr166His	18662576	missense	exon 5 of 6 position 170 of 196 (coding)	NA
RS1	c.498C>G	p.Tyr166*	18662574	nonsense	exon 5 of 6 position 172 of 196 (coding)	NA
RS1	c.508A>C	p.Thr170Pro	18662564	missense	exon 5 of 6 position 182 of 196 (coding)	NA
RS1	c.515del	p.Asn172Thrfs*65	18662557	frameshift	exon 5 of 6 position 189 of 196 (splicing, coding, NMD)	NA
RS1	c.544C>T	p.Arg182Cys	18660255	missense	exon 6 of 6 position 22 of 2469 (coding)	rs61753171
RS1	c.554C>A	p.Thr185Lys	18660245	missense	exon 6 of 6 position 32 of 2469 (coding)	NA
RS1	c.574_580delinsACCCCCCT	p.Pro192Thrfs*72	18660219	frameshift	exon 6 of 6 position 52-58 of 2469 (coding, NMD)	NA
RS1	c.574C>T	p.Pro192Ser	18660225	missense	exon 6 of 6 position 52 of 2469 (coding)	rs61753174
RS1	c.575C>T	p.Pro192Leu	18660224	missense	exon 6 of 6 position 53 of 2469 (coding)	NA
RS1	c.577C>T	p.Pro193Ser	18660222	missense	exon 6 of 6 position 55 of 2469 (coding)	rs281865351
RS1	c.579dup	p.Ile194Hisfs*70	18660220	frameshift	exon 6 of 6 before position 58 of 2469 (coding, NMD)	rs199469697
RS1	c.589C>T	p.Arg197Cys	18660210	missense	exon 6 of 6 position 67 of 2469 (coding)	rs281865354
RS1	c.590G>A	p.Arg197His	18660209	missense	exon 6 of 6 position 68 of 2469 (coding)	rs281865355
RS1	c.596T>A	p.Ile199Asn	18660203	missense	exon 6 of 6 position 74 of 2469 (coding)	NA
RS1	c.596T>C	p.Ile199Thr	18660203	missense	exon 6 of 6 position 74 of 2469 (coding)	rs281865356
RS1	c.598C>T	p.Arg200Cys	18660201	missense	exon 6 of 6 position 76 of 2469 (coding)	rs281865357
RS1	c.598C>A	p.Arg200Ser	18660201	missense	exon 6 of 6 position 76 of 2469 (coding)	NA
RS1	c.599G>A	p.Arg200His	18660200	missense	exon 6 of 6 position 77 of 2469 (coding)	rs281865358
RS1	c.608C>T	p.Pro203Leu	18660191	missense	exon 6 of 6 position 86 of 2469 (coding)	rs104894930
RS1	c.625C>T	p.Arg209Cys	18660174	missense	exon 6 of 6 position 103 of 2469 (coding)	rs281865361
RS1	c.637C>T	p.Arg213Trp	18660162	missense	exon 6 of 6 position 115 of 2469 (coding)	rs281865365
RS1	c.638G>A	p.Arg213Gln	18660161	missense	exon 6 of 6 position 116 of 2469 (coding)	rs281865364
RS1	c.647T>C	p.Leu216Pro	18660152	missense	exon 6 of 6 position 125 of 2469 (coding)	rs281865368
RS1	c.(?_1-1)_(52+1_53-1)del					
RS1	c.(184+1_185-1)_(522+1_523-1)del					
RS1	c.(52+1_53-1)_(184+1_185-1)del					
RS1	c.(52+1_53-1)_(78+1_79-1)del					

Variants in bold are novel

Exonic deletions are described based on the edge positions of exons.

Reference: NM_000330.4; ENST00000379984; GRCh37.p13.

The previously reported variants were surveyed with the HGMD database (<https://portal.biobase-international.com>; accessed on 1st December 2020).

Supplementary Table 2: Pathogenicity Assessment

Gene	Nucleotide change	Amino acid change	Verdict	ACMG Classification															
				Identified classification rules															
				Factor 1	Factor 2	Factor 3	Factor 4	Factor 5	Factor 6	Factor 7	Factor 8	Factor 9							
RS1	c.20del	p.Gly7Alafs*119	Pathogenic	PVS1	PM2	PP3	PP4												
RS1	c.35T>A	p.Leu12His	Likely Pathogenic	PM1	PM2	PP2	PP3	PP4	PP5										
RS1	c.52+1G>T		Pathogenic	PVS1	PM2	PP3	PP4												
RS1	c.52+2T>C		Pathogenic	PVS1	PM2	PP3	PP4												
RS1	c.52+5G>C		Uncertain Significance	PM2	PP4														
RS1	c.53-34A>G		Uncertain Significance	PM2	PP4	BP4													
RS1	c.78G>C	p.Glu26Asp	Likely Pathogenic	PVS1	PM2	PP2	PP3	PP4											
RS1	c.103C>T	p.Gln35*	Pathogenic	PVS1	PM2	PP3													
RS1	c.120C>A	p.Cys40*	Pathogenic	PVS1	PM2	PP4	BP4												
RS1	c.184+2T>G		Pathogenic	PVS1	PM2	PP3	PP4	PP5											
RS1	c.185-1G>A		Pathogenic	PVS1	PM2	PP3	PP4												
RS1	c.206T>C	p.Leu69Pro	Likely Pathogenic	PM1	PM2	PP2	PP3	PP4											
RS1	c.209G>A	p.Gly70Asp	Likely Pathogenic	PM1	PM2	PM5	PP2	PP3	PP4										
RS1	c.214G>C	p.Glu72Gln	Pathogenic	PM1	PM2	PM5	PP2	PP3	PP4										
RS1	c.214G>A	p.Glu72Lys	Pathogenic	PM1	PM2	PM5	PP1	PP2	PP3	PP4	PP5								
RS1	c.216G>C	p.Glu72Asp	Pathogenic	PS1	PM1	PM2	PP1	PP2	PP3	PP4	PP5								
RS1	c.239A>C	p.Gln80Pro	Likely Pathogenic	PM1	PM2	PP2	PP3	PP4											
RS1	c.242T>A	p.Ile81Asn	Likely Pathogenic	PM1	PM2	PP2	PP3	PP4											
RS1	c.276G>C	p.Trp92Cys	Likely Pathogenic	PM1	PM2	PP2	PP3	PP4	PP5										
RS1	c.288G>C	p.Trp96Cys	Likely Pathogenic	PM1	PM2	PM5	PP2	PP3	PP4	PP5									
RS1	c.304C>T	p.Arg102Trp	Likely Pathogenic	PM1	PM2	PM5	PP1	PP2	PP3	PP4	PP5								
RS1	c.305G>A	p.Arg102Gln	Pathogenic	PM1	PM2	PM5	PP1	PP2	PP3	PP4	PP5								
RS1	c.308T>G	p.Leu103Arg	Likely Pathogenic	PM1	PM2	PP1	PP2	PP3	PP4	PP5									
RS1	c.317A>C	p.Gln106Pro	Likely Pathogenic	PM1	PM2	PP2	PP3	PP4											
RS1	c.325G>C	p.Gly109Arg	Pathogenic	PS1	PM1	PM2	PM5	PP1	PP2	PP3	PP4	PP5							
RS1	c.325G>T	p.Gly109Trp	Pathogenic	PS1	PM1	PM2	PM5	PP1	PP2	PP3	PP4	PP5							
RS1	c.326+1G>A		Pathogenic	PVS1	PM2	PP3	PP4												
RS1	c.326G>C	p.Gly109Ala	Pathogenic	PVS1	PM2	PM5	PM2	PP3	PP4										
RS1	c.329G>A	p.Cys110Tyr	Likely Pathogenic	PM1	PM2	PP1	PP2	PP3	PP4	PP5									
RS1	c.336_337delinsTT	p.Trp112_Leu113del	Likely Pathogenic	PM1	PM2	PP3	PP4												
RS1	c.337C>T	p.Leu113Phe	Likely Pathogenic	PM1	PM2	PP2	PP3	PP4	PP5										
RS1	c.349C>T	p.Gln117*	Pathogenic	PVS1	PM2	PP3	PP4												
RS1	c.378del	p.Leu127*	Pathogenic	PVS1	PM2	PP4													
RS1	c.421C>T	p.Arg141Cys	Pathogenic	PM1	PM2	PM5	PP1	PP2	PP3	PP4	PP5								
RS1	c.422G>A	p.Arg141His	Pathogenic	PM1	PM2	PM5	PP1	PP2	PP3	PP4	PP5								
RS1	c.422G>T	p.Arg141Leu	Pathogenic	PM1	PM2	PM5	PP2	PP3	PP4										
RS1	c.435dup	p.Ile146AsnfsTer15	Pathogenic	PVS1	PM2	PP3	PP4												
RS1	c.438G>C	p.Glu146Asp	Pathogenic	PS1	PM1	PM2	PM5	PP1	PP2	PP3	PP4	PP5							
RS1	c.496_498del	p.Tyr166del	Likely Pathogenic	PM1	PM2	PM4	PP3	PP4											
RS1	c.496T>C	p.Tyr166His	Likely Pathogenic	PM1	PM2	PP2	PP3	PP4											
RS1	c.498C>G	p.Tyr166*	Pathogenic	PVS1	PM2	PP3	PP4												
RS1	c.508A>C	p.Thr170Pro	Likely Pathogenic	PM1	PM2	PP2	PP3	PP4											
RS1	c.515del	p.Asn172Thrfs*65	Pathogenic	PVS1	PM2	PP3	PP4												
RS1	c.544C>T	p.Arg182Cys	Likely Pathogenic	PM1	PM2	PP2	PP3	PP4	PP5										
RS1	c.554C>A	p.Thr185Lys	Likely Pathogenic	PM1	PM2	PP2	PP3	PP4											
RS1	c.574_580delinsACCCCCCT	p.Pro192Thrfs*72	Pathogenic	PVS1	PM2	PP3	PP4												
RS1	c.574C>T	p.Pro192Ser	Pathogenic	PS1	PM1	PM2	PM5	PP1	PP2	PP3	PP4	PP5							
RS1	c.575C>T	p.Pro192Leu	Pathogenic	PM1	PM2	PM5	PM2	PP3	PP4										
RS1	c.577C>T	p.Pro193Ser	Pathogenic	PS1	PM1	PM2	PM5	PP2	PP3	PP4	PP5								
RS1	c.579dup	p.Ile194Hisfs*70	Pathogenic	PVS1	PM2	PP1	PP3	PP4	PP5										
RS1	c.589C>T	p.Arg197Cys	Pathogenic	PM1	PM2	PM5	PP1	PP2	PP3	PP4	PP5								
RS1	c.590G>A	p.Arg197His	Pathogenic	PM1	PM2	PM5	PP2	PP3	PP4	PP5									
RS1	c.596T>A	p.Ile199Asn	Likely Pathogenic	PM1	PM2	PM5	PP2	PP3	PP4										
RS1	c.596T>C	p.Ile199Thr	Likely Pathogenic	PM1	PM2	PP1	PP2	PP3	PP4	PP5									
RS1	c.598C>T	p.Arg200Cys	Pathogenic	PM1	PM2	PM5	PP1	PP2	PP3	PP4	PP5								
RS1	c.598C>A	p.Arg200Ser	Likely Pathogenic	PM1	PM2	PM5	PP1	PP2	PP3	PP4									
RS1	c.599G>A	p.Arg200His	Pathogenic	PM1	PM2	PM5	PP1	PP2	PP3	PP4	PP5								
RS1	c.608C>T	p.Pro203Leu	Pathogenic	PM1	PM2	PM5	PP1	PP2	PP3	PP4	PP5								
RS1	c.625C>T	p.Arg209Cys	Pathogenic	PM1	PM2	PM5	PP1	PP2	PP3	PP4	PP5								
RS1	c.637C>T	p.Arg213Trp	Pathogenic	PM1	PM2	PM5	PP1	PP2	PP3	PP4	PP5								
RS1	c.638G>A	p.Arg213Gln	Pathogenic	PM1	PM2	PM5	PP1	PP2	PP3	PP4	PP5								
RS1	c.647T>C	p.Leu216Pro	Pathogenic	PM1	PM2	PP2	PP3	PP4	PP5										
RS1	c.(?_1-1)_(52+1_53-1)del																		
RS1	c.(184+1_185-1)_(522+1_523-1)del																		
RS1	c.(52+1_53-1)_(184+1_185-1)del																		
RS1	c.(52+1_53-1)_(78+1_79-1)del																		

Assessment of pathogenicity was performed based on the American College of Medical Genetics and Genomics (ACMG) guidelines.

Supplementary Table 3: Allele Frequency

Gene	Nucleotide change	Amino acid change	GnomAD allele frequency													Coverage in GnomAD Exomes samples		
			Allele frequency (exome)						Allele frequency (genome)						Mean coverage	Median coverage	% of samples over 20x coverage	
			East Asian	South Asian	African	European (Non-Finnish)	Latino	Total	East Asian	South Asian	African	European (Non-Finnish)	Total					
RS1	c.20del	p.Gly7Alafs*119	NA	NA	NA	NA	NA	NA	NA	NA	NA	NA	NA	70.9	72	99.70%		
RS1	c.35T>A	p.Leu12His	NA	NA	NA	NA	NA	NA	NA	NA	NA	NA	NA	70.9	72	99.63%		
RS1	c.52+1G>T		NA	NA	NA	NA	NA	NA	NA	NA	NA	NA	NA	68.2	68	98.85%		
RS1	c.52+2T>C		NA	NA	NA	NA	NA	NA	NA	NA	NA	NA	NA	68.1	68	98.71%		
RS1	c.52+5G>C		NA	NA	NA	NA	NA	NA	NA	NA	NA	NA	NA	68.2	67	98.87%		
RS1	c.53-34A>G		NA	NA	NA	NA	NA	NA	NA	NA	NA	NA	NA	46.6	43	93.64%		
RS1	c.78G>C	p.Glu26Asp	NA	NA	NA	NA	NA	NA	NA	NA	NA	NA	NA	58.5	56	98.79%		
RS1	c.103C>T	p.Gln35*	NA	NA	NA	NA	NA	NA	NA	NA	NA	NA	NA	91.8	100	99.97%		
RS1	c.120C>A	p.Cys40*	NA	NA	NA	NA	NA	NA	NA	NA	NA	NA	NA	94.6	100	99.99%		
RS1	c.184+2T>G		NA	NA	NA	NA	NA	NA	NA	NA	NA	NA	NA	90.2	100	99.93%		
RS1	c.185-1G>A		NA	NA	NA	NA	NA	NA	NA	NA	NA	NA	NA	67.5	68	99.06%		
RS1	c.206T>C	p.Leu69Pro	NA	NA	NA	NA	NA	NA	NA	NA	NA	NA	NA	71.3	72	99.44%		
RS1	c.209G>A	p.Gly70Asp	NA	NA	NA	NA	NA	NA	NA	NA	NA	NA	NA	71.6	73	99.44%		
RS1	c.214G>C	p.Glu72Gln	NA	NA	NA	NA	NA	NA	NA	NA	NA	NA	NA	71.3	73	99.51%		
RS1	c.214G>A	p.Glu72Lys	NA	NA	NA	NA	NA	NA	NA	NA	NA	NA	NA	71.3	73	99.51%		
RS1	c.216G>C	p.Glu72Asp	NA	NA	NA	NA	NA	NA	NA	NA	NA	NA	NA	73.1	75	99.52%		
RS1	c.239A>C	p.Gln80Pro	NA	NA	NA	NA	NA	NA	NA	NA	NA	NA	NA	74.3	78	99.53%		
RS1	c.242T>A	p.Ile81Asn	NA	NA	NA	NA	NA	NA	NA	NA	NA	NA	NA	74.5	78	99.52%		
RS1	c.276G>C	p.Trp92Cys	NA	NA	NA	NA	NA	NA	NA	NA	NA	NA	NA	79.2	87	99.53%		
RS1	c.288G>C	p.Trp96Cys	NA	NA	NA	NA	NA	NA	NA	NA	NA	NA	NA	78.2	85	99.50%		
RS1	c.304C>T	p.Arg102Trp	0.0000722	NA	NA	NA	NA	0.00000546	NA	NA	NA	NA	NA	74.7	78	99.46%		
RS1	c.305G>A	p.Arg102Gln	NA	NA	NA	0.0000122	NA	0.00000546	NA	NA	NA	NA	NA	74.4	77	99.43%		
RS1	c.308T>G	p.Leu103Arg	NA	NA	NA	NA	NA	NA	NA	NA	NA	NA	NA	73.8	76	99.41%		
RS1	c.317A>C	p.Gln106Pro	NA	NA	NA	NA	NA	NA	NA	NA	NA	NA	NA	72.4	74	99.35%		
RS1	c.325G>C	p.Gly109Arg	NA	NA	NA	0.000188	NA	0.0000164	NA	NA	NA	NA	NA	69.4	70	99.21%		
RS1	c.325G>T	p.Gly109Trp	NA	NA	NA	NA	NA	0.0000164	NA	NA	NA	NA	NA	69.4	70	99.21%		
RS1	c.326+1G>A		NA	NA	NA	NA	NA	NA	NA	NA	NA	NA	NA	68.9	69	99.10%		
RS1	c.326G>C	p.Gly109Ala	NA	NA	NA	NA	NA	NA	NA	NA	NA	NA	NA	69.1	69	99.15%		
RS1	c.329G>A	p.Cys110Tyr	NA	NA	NA	NA	NA	NA	NA	NA	NA	NA	NA	74	80	99.51%		
RS1	c.336_337delinsTT	p.Trp112_Leu113del	NA	NA	NA	NA	NA	NA	NA	NA	NA	NA	NA	75.3	81	99.65%		
RS1	c.337C>T	p.Leu113Phe	NA	NA	NA	NA	NA	NA	NA	NA	NA	NA	NA	75.3	81	99.65%		
RS1	c.349C>T	p.Gln117*	NA	NA	NA	NA	NA	NA	NA	NA	NA	NA	NA	79.6	88	99.81%		
RS1	c.378del	p.Leu127*	NA	NA	NA	NA	NA	NA	NA	NA	NA	NA	NA	86.7	100	99.97%		
RS1	c.421C>T	p.Arg141Cys	NA	NA	NA	NA	NA	NA	NA	NA	NA	NA	NA	91.2	100	100%		
RS1	c.422G>A	p.Arg141His	NA	NA	NA	NA	NA	NA	NA	NA	NA	NA	NA	91.3	100	100%		
RS1	c.422G>T	p.Arg141Leu	NA	NA	NA	NA	NA	NA	NA	NA	NA	NA	NA	91.3	100	100%		
RS1	c.435dup	p.Ile146AsnfsTer15	NA	NA	NA	NA	NA	NA	NA	NA	NA	NA	NA	91.8	100	99.98%		
RS1	c.438G>C	p.Glu146Asp	NA	NA	NA	NA	NA	NA	NA	NA	NA	NA	NA	91.7	100	99.98%		
RS1	c.496_498del	p.Tyr166del	NA	NA	NA	NA	NA	NA	NA	NA	NA	NA	NA	87.9	100	99.96%		
RS1	c.496T>C	p.Tyr166His	NA	NA	NA	NA	NA	NA	NA	NA	NA	NA	NA	88.1	100	99.97%		
RS1	c.498C>G	p.Tyr166*	NA	NA	NA	NA	NA	NA	NA	NA	NA	NA	NA	87.9	100	99.96%		
RS1	c.508A>C	p.Thr170Pro	NA	NA	NA	NA	NA	NA	NA	NA	NA	NA	NA	87.2	100	99.88%		
RS1	c.515del	p.Asn172Thrfs*65	NA	NA	NA	NA	NA	NA	NA	NA	NA	NA	NA	86.2	100	99.90%		
RS1	c.544C>T	p.Arg182Cys	NA	NA	NA	NA	NA	0.00000548	NA	NA	NA	NA	NA	73.5	75	99.61%		
RS1	c.554C>A	p.Thr185Lys	NA	NA	NA	NA	NA	NA	NA	NA	NA	NA	NA	76	79	99.62%		
RS1	c.574_580delinsACCCCCCT	p.Pro192Thrfs*72	NA	NA	NA	NA	NA	NA	NA	NA	NA	NA	NA	77.6	81	99.59%		
RS1	c.574C>T	p.Pro192Ser	NA	NA	NA	NA	NA	NA	NA	NA	NA	NA	NA	76.3	79	99.59%		
RS1	c.575C>T	p.Pro192Leu	NA	NA	NA	NA	NA	NA	NA	NA	NA	NA	NA	76.7	80	99.59%		
RS1	c.577C>T	p.Pro193Ser	NA	NA	NA	NA	NA	NA	NA	NA	NA	NA	NA	77.6	81	99.59%		
RS1	c.579dup	p.Ile194Hisfs*70	NA	NA	NA	NA	NA	NA	NA	NA	NA	NA	NA	77.6	81	99.59%		
RS1	c.589C>T	p.Arg197Cys	NA	NA	NA	NA	NA	NA	NA	NA	NA	NA	NA	78.9	83	99.61%		
RS1	c.590G>A	p.Arg197His	NA	NA	NA	NA	NA	0.00000546	NA	NA	NA	NA	NA	78.5	83	99.58%		
RS1	c.596T>A	p.Ile199Asn	NA	NA	NA	NA	NA	NA	NA	NA	NA	NA	NA	78.4	82	99.56%		
RS1	c.596T>C	p.Ile199Thr	NA	NA	NA	NA	NA	NA	NA	NA	NA	NA	NA	78.4	82	99.56%		
RS1	c.598C>T	p.Arg200Cys	NA	NA	NA	NA	NA	NA	NA	NA	NA	NA	NA	78.8	83	99.58%		
RS1	c.598C>A	p.Arg200Ser	NA	NA	NA	NA	NA	NA	NA	NA	NA	NA	NA	78.8	83	99.58%		
RS1	c.599G>A	p.Arg200His	NA	NA	NA	NA	NA	NA	NA	NA	NA	NA	NA	78.7	83	99.55%		
RS1	c.608C>T	p.Pro203Leu	NA	NA	NA	NA	NA	NA	NA	NA	NA	NA	NA	78.9	86	99.43%		
RS1	c.625C>T	p.Arg209Cys	NA	NA	NA	NA	NA	NA	NA	NA	NA	NA	NA	78.9	84	99.48%		
RS1	c.637C>T	p.Arg213Trp	NA	NA	NA	NA	NA	NA	NA	NA	NA	NA	NA	77.3	84	99.25%		
RS1	c.638G>A	p.Arg213Gln	NA	NA	NA	NA	NA	NA	NA	NA	NA	NA	NA	77.3	84	99.23%		
RS1	c.647T>C	p.Leu216Pro	NA	NA	NA	NA	NA	NA	NA	NA	NA	NA	NA	77.8	87	99.12%		
RS1	c.(?_1-1)_(52+1_53-1)del																	
RS1	c.(184+1_185-1)_(522+1_523-1)del																	
RS1	c.(52+1_53-1)_(184+1_185-1)del																	
RS1	c.(52+1_53-1)_(78+1_79-1)del																	

NA=not available.

Exonic deletions are described based on the edge positions of exons.

The allelic frequency was investigated on the public databases (<http://gnomad.broadinstitute.org/>; <http://sites.google.com/site/popgen/dbNSFP>).

The population data and general coverage by whole-genome sequencing was provided with the GnomAD database. (<http://gnomad.broadinstitute.org/>).

Supplementary Table 4: General Prediction

Gene	Nucleotide change	Amino acid change	Verdict	General prediction									
				MutationTaster			FATHMM		CADD		REVEL		
				Prediction	Accuracy	Converted rankscore	Prediction	Score	Converted rankscore	Score	Prediction	Score	Rankscore
RS1	c.20del	p.Gly7Alafs*119	Pathogenic	NA	NA	NA	NA	NA	NA	NA	NA	NA	NA
RS1	c.35T>A	p.Leu12His	Likely Pathogenic	Polymorphism	0.7844	0.2929	Damaging	-5.16	0.9879	25.6	Pathogenic	0.633	0.8609
RS1	c.52+1G>T		Pathogenic	Disease causing	1	0.81	NA	NA	NA	32	NA	NA	NA
RS1	c.52+2T>C		Pathogenic	Disease causing	1	0.81	NA	NA	NA	31	NA	NA	NA
RS1	c.52+5G>C		Uncertain Significance	NA	NA	NA	NA	NA	NA	23.2	NA	NA	NA
RS1	c.53-34A>G		Uncertain Significance	NA	NA	NA	NA	NA	NA	8.719	NA	NA	NA
RS1	c.78G>C	p.Glu26Asp	Likely Pathogenic	Polymorphism	0.7924	0.2921	Damaging	-4.89	0.9831	20.2	Benign	0.4259	0.7366
RS1	c.103C>T	p.Gln35*	Pathogenic	Disease causing	1	0.81	NA	NA	NA	35	NA	NA	NA
RS1	c.120C>A	p.Cys40*	Pathogenic	Disease causing	1	0.81	NA	NA	NA	16.67	NA	NA	NA
RS1	c.184+2T>G		Pathogenic	Disease causing	1	0.81	NA	NA	NA	25.8	NA	NA	NA
RS1	c.185-1G>A		Pathogenic	Disease causing	1	0.81	NA	NA	NA	34	NA	NA	NA
RS1	c.206T>C	p.Leu69Pro	Likely Pathogenic	Disease causing	1	0.81	Damaging	-5.73	0.993	27.7	Pathogenic	0.976	0.9979
RS1	c.209G>A	p.Gly70Asp	Likely Pathogenic	Disease causing	1	0.81	Damaging	-5.78	0.9936	27.2	Pathogenic	0.985	0.9993
RS1	c.214G>C	p.Glu72Gln	Pathogenic	Disease causing	1	0.81	Damaging	-5.41	0.9908	26.5	Pathogenic	0.9309	0.984
RS1	c.214G>A	p.Glu72Lys	Pathogenic	Disease causing	1	0.81	Damaging	-5.4	0.9907	25.7	Pathogenic	0.921	0.9803
RS1	c.216G>C	p.Glu72Asp	Pathogenic	Disease causing	1	0.81	Damaging	-5.44	0.9909	23.2	Pathogenic	0.93	0.9837
RS1	c.239A>C	p.Gln80Pro	Likely Pathogenic	Disease causing	1	0.81	Damaging	-5.53	0.9918	26.4	Pathogenic	0.971	0.9968
RS1	c.242T>A	p.Ile81Asn	Likely Pathogenic	Disease causing	1	0.81	Damaging	-5.19	0.9864	27.7	Pathogenic	0.962	0.9944
RS1	c.276G>C	p.Trp92Cys	Likely Pathogenic	Disease causing	1	0.81	Damaging	-4.78	0.9814	32	Pathogenic	0.9819	0.9899
RS1	c.288G>C	p.Trp96Cys	Likely Pathogenic	Disease causing	1	0.81	Damaging	-5.37	0.9904	32	Pathogenic	0.938	0.9866
RS1	c.304C>T	p.Arg102Trp	Likely Pathogenic	Disease causing	1	0.81	Damaging	-4.99	0.9851	25.4	Pathogenic	0.958	0.9933
RS1	c.305G>A	p.Arg102Gln	Pathogenic	Disease causing	1	0.81	Damaging	-4.97	0.9847	29.7	Pathogenic	0.9829	0.9991
RS1	c.308T>G	p.Leu103Arg	Likely Pathogenic	Disease causing	1	0.81	Damaging	-5.08	0.9867	29.7	Pathogenic	0.985	0.9993
RS1	c.317A>C	p.Gln106Pro	Likely Pathogenic	Disease causing	1	0.81	Damaging	-4.84	0.9823	27.2	Pathogenic	0.8439	0.9521
RS1	c.325G>C	p.Gly109Arg	Pathogenic	Disease causing	1	0.81	Damaging	-4.85	0.9825	34	Pathogenic	0.8679	0.9608
RS1	c.325G>T	p.Gly109Trp	Pathogenic	Disease causing	1	0.81	Damaging	-4.85	0.9825	34	Pathogenic	0.8679	0.9608
RS1	c.326+1G>A		Pathogenic	Disease causing	1	0.81	NA	NA	NA	28	NA	NA	NA
RS1	c.326G>C	p.Gly109Ala	Pathogenic	Disease causing	1	0.81	Damaging	-4.81	0.9818	34	Pathogenic	0.74	0.911
RS1	c.329G>A	p.Cys110Tyr	Likely Pathogenic	Disease causing	1	0.81	Damaging	-4.76	0.9811	24.8	Pathogenic	0.882	0.9659
RS1	c.336_337delinsTT	p.Trp112_Leu113delinsCysPhe	Likely Pathogenic	NA	NA	NA	NA	NA	NA	26.4	NA	NA	NA
RS1	c.337C>T	p.Leu113Phe	Likely Pathogenic	Disease causing	1	0.81	Damaging	-4.79	0.9815	NA	Pathogenic	0.874	0.9629
RS1	c.349C>T	p.Gln117*	Pathogenic	Disease causing	1	0.81	NA	NA	NA	38	NA	NA	NA
RS1	c.378del	p.Leu127*	Pathogenic	Disease causing	1	0.81	NA	NA	NA	NA	NA	NA	NA
RS1	c.421C>T	p.Arg141Cys	Pathogenic	Disease causing	1	0.81	Damaging	-5.2	0.9885	32	Pathogenic	0.8169	0.942
RS1	c.422G>A	p.Arg141His	Pathogenic	Disease causing	1	0.81	Damaging	-5.2	0.9885	29.5	Pathogenic	0.9089	0.9759
RS1	c.422G>T	p.Arg141Leu	Pathogenic	Disease causing	1	0.81	Damaging	-5.19	0.9884	31	Pathogenic	0.939	0.9869
RS1	c.435dup	p.Ile146AsnfsTer15	Pathogenic	NA	NA	NA	NA	NA	NA	NA	NA	NA	NA
RS1	c.438G>C	p.Glu146Asp	Pathogenic	Disease causing	1	0.81	Damaging	-4.78	0.9814	23.7	Pathogenic	0.7699	0.9236
RS1	c.496_498del	p.Tyr166del	Likely Pathogenic	NA	NA	NA	NA	NA	NA	27.6	NA	NA	NA
RS1	c.496T>C	p.Tyr166His	Likely Pathogenic	Disease causing	1	0.81	Damaging	-4.95	0.9843	35	Pathogenic	0.9409	0.9876
RS1	c.498C>G	p.Tyr166*	Pathogenic	Disease causing	1	0.81	NA	NA	NA	20.8	NA	NA	NA
RS1	c.508A>C	p.Thr170Pro	Likely Pathogenic	Disease causing	1	0.81	Damaging	-5.31	0.9898	26.9	Pathogenic	0.8519	0.9549
RS1	c.515del	p.Asn172Thrfs*65	Pathogenic	NA	NA	NA	NA	NA	NA	NA	NA	NA	NA
RS1	c.544C>T	p.Arg182Cys	Likely Pathogenic	Disease causing	1	0.81	Damaging	-4.81	0.9818	25.4	Pathogenic	0.9179	0.9792
RS1	c.554C>A	p.Thr185Lys	Likely Pathogenic	Disease causing	1	0.81	Damaging	-5.21	0.9887	23.8	Pathogenic	0.753	0.9165
RS1	c.574_580delinsACCCCCCT	p.Pro192Thrfs*72	Pathogenic	NA	NA	NA	NA	NA	NA	27.4	NA	NA	NA
RS1	c.574C>T	p.Pro192Ser	Pathogenic	Disease causing	1	0.81	Damaging	-4.89	0.9831	29.4	Pathogenic	0.9459	0.9894
RS1	c.575C>T	p.Pro192Leu	Pathogenic	Disease causing	1	0.81	Damaging	-4.93	0.9839	35	Pathogenic	0.9629	0.9947
RS1	c.577C>T	p.Pro193Ser	Pathogenic	Disease causing	1	0.81	Damaging	-5.13	0.9875	27.4	Pathogenic	0.9589	0.9936
RS1	c.579dup	p.Ile194Hisfs*70	Pathogenic	NA	NA	NA	NA	NA	NA	NA	NA	NA	NA
RS1	c.589C>T	p.Arg197Cys	Pathogenic	Disease causing	1	0.81	Damaging	-6.58	0.9973	34	Pathogenic	0.99	0.9998
RS1	c.590G>A	p.Arg197His	Pathogenic	Disease causing	1	0.81	Damaging	-6.56	0.9973	32	Pathogenic	0.984	0.9992
RS1	c.596T>A	p.Ile199Asn	Likely Pathogenic	Disease causing	1	0.81	Damaging	-5.32	0.9899	26.6	Pathogenic	0.972	0.9969
RS1	c.596T>C	p.Ile199Thr	Likely Pathogenic	Disease causing	1	0.81	Damaging	-5.32	0.9899	29	Pathogenic	0.957	0.9929
RS1	c.598C>T	p.Arg200Cys	Pathogenic	Disease causing	1	0.81	Damaging	-6.75	0.9979	28.3	Pathogenic	0.944	0.9887
RS1	c.598C>A	p.Arg200Ser	Likely Pathogenic	Disease causing	1	0.81	Damaging	-6.73	0.9978	29.3	Pathogenic	0.925	0.9818
RS1	c.599G>A	p.Arg200His	Pathogenic	Disease causing	1	0.81	Damaging	-6.74	0.9978	33	Pathogenic	0.986	0.9994
RS1	c.608C>T	p.Pro203Leu	Pathogenic	Disease causing	1	0.81	Damaging	-5.61	0.9923	31	Pathogenic	0.981	0.9988
RS1	c.625C>T	p.Arg209Cys	Pathogenic	Disease causing	1	0.81	Damaging	-5.34	0.9901	34	Pathogenic	0.9549	0.9923
RS1	c.637C>T	p.Arg213Trp	Pathogenic	Disease causing	1	0.81	Damaging	-5.04	0.9859	31	Pathogenic	0.967	0.9958
RS1	c.638G>A	p.Arg213Gln	Pathogenic	Disease causing	1	0.81	Damaging	-5.06	0.9863	33	Pathogenic	0.985	0.9993
RS1	c.647T>C	p.Leu216Pro	Pathogenic	Disease causing	1	0.81	Damaging	-5.85	0.994	29.7	Pathogenic	0.9689	0.9963
RS1	c.(?_1-1)_(52+1_53-1)del												
RS1	c.(184+1_185-1)_(522+1_523-1)del												
RS1	c.(52+1_53-1)_(184+1_185-1)del												
RS1	c.(52+1_53-1)_(78+1_79-1)del												

NA=not available.

Exonic deletions are described based on the edge positions of exons.

Reference: NM_000330.4; ENST00000379984; GRCh37.p13.

MutationTaster (<http://www.mutationtaster.org/>), FATHMM (<http://fathmm.biocompute.org.uk/>),SIFT (<https://www.sift.co.uk/>), PROVEAN (<http://provean.jcvi.org/index.php>),Polyphen 2 (<http://genetics.bwh.harvard.edu/pph2/>), Revel (<https://labworm.com/tool/revel>), CADD (<https://cadd.gs.washington.edu/info>),Human splicing finder, HSF(<http://www.umd.be/HSF3/>), ClinVar (<https://www.ncbi.nlm.nih.gov/clinvar/>).

Supplementary Table 5: Functional Prediction

Gene	Nucleotide change	Amino acid change	Functional prediction								
			SIFT			PROVEAN			Polyphen2		Human Splice Finder 3.0
			Prediction	Score	Converted rankscore	Prediction	Score	Converted rankscore	Prediction	Score	
RS1	c.20del	p.Gly7Alafs*119	NA	NA	NA	NA	NA	NA	NA	NA	Potential alteration of splicing
RS1	c.35T>A	p.Leu12His	Damaging	0.001	0.7849	Neutral	0.23	NA	possibly_damaging	0.667	No significant impact on splicing signals.
RS1	c.52+1G>T		NA	NA	NA	NA	NA	NA	NA	NA	Most probably affecting splicing
RS1	c.52+2T>C		NA	NA	NA	NA	NA	NA	NA	NA	Most probably affecting splicing
RS1	c.52+5G>C		NA	NA	NA	NA	NA	NA	NA	NA	Most probably affecting splicing
RS1	c.53-34A>G		NA	NA	NA	NA	NA	NA	NA	NA	Potential alteration of splicing
RS1	c.78G>C	p.Glu26Asp	Tolerated	0.204	0.2008	Neutral	-1.39	benign		0.05	Most probably affecting splicing
RS1	c.103C>T	p.Gln35*	NA	NA	NA	NA	NA	NA	NA	NA	No significant impact on splicing signals.
RS1	c.120C>A	p.Cys40*	NA	NA	NA	NA	NA	NA	NA	NA	Potential alteration of splicing
RS1	c.184+2T>G		NA	NA	NA	NA	NA	NA	NA	NA	Most probably affecting splicing
RS1	c.185-1G>A		NA	NA	NA	NA	NA	NA	NA	NA	Most probably affecting splicing
RS1	c.206T>C	p.Leu69Pro	Damaging	0	0.9125	Damaging	-6.68	0.9239	probably_damaging	0.936	No significant impact on splicing signals.
RS1	c.209G>C	p.Gly70Asp	Damaging	0	0.9125	Damaging	-6.83	0.9302	probably_damaging	0.999	No significant impact on splicing signals.
RS1	c.214G>A	p.Glu72Gln	Damaging	0.005	0.6323	Damaging	-2.8	0.5923	probably_damaging	0.998	No significant impact on splicing signals.
RS1	c.214G>A	p.Glu72Lys	Tolerated	0.264	0.1636	Damaging	-3.65	0.6995	probably_damaging	0.999	Potential alteration of splicing
RS1	c.216G>C	p.Glu72Asp	Damaging	0.009	0.5748	Damaging	-2.85	0.6003	probably_damaging	0.991	Potential alteration of splicing
RS1	c.239A>C	p.Gln80Pro	Damaging	0.006	0.6144	Damaging	-5.05	0.827	probably_damaging	0.999	Significant alteration of exonic splicing enhancer / Exonic splicing silencer motifs ratio
RS1	c.242T>A	p.Ile81Asn	Damaging	0	0.9125	Damaging	-6.64	0.9222	probably_damaging	0.972	No significant impact on splicing signals.
RS1	c.276G>C	p.Trp62Cys	Damaging	0.016	0.5185	Damaging	-7.56	0.9522	probably_damaging	1	No significant impact on splicing signals.
RS1	c.288G>C	p.Trp96Cys	Damaging	0.044	0.4109	Damaging	-10.64	0.9913	probably_damaging	1	Potential alteration of splicing
RS1	c.304C>T	p.Arg102Trp	Damaging	0.005	0.6323	Damaging	-7.77	0.9584	probably_damaging	1	Potential alteration of splicing
RS1	c.305G>A	p.Arg102Gln	Damaging	0.004	0.6542	Damaging	-3.9	0.7293	probably_damaging	0.998	No significant impact on splicing signals.
RS1	c.308T>G	p.Leu103Arg	Damaging	0	0.9125	Damaging	-5.84	0.8843	probably_damaging	1	No significant impact on splicing signals.
RS1	c.317A>C	p.Gln106Pro	Tolerated	0.054	0.3863	Damaging	-4.19	0.7562	probably_damaging	0.999	Significant alteration of exonic splicing enhancer / Exonic splicing silencer motifs ratio
RS1	c.325G>C	p.Gly109Arg	Damaging	0.009	0.6676	Damaging	-2.86	0.6019	probably_damaging	1	Significant alteration of exonic splicing enhancer / Exonic splicing silencer motifs ratio
RS1	c.325G>T	p.Gly109Trp	Damaging	0.009	0.6676	Damaging	-2.86	0.6019	probably_damaging	1	No significant impact on splicing signals.
RS1	c.326+1G>A		NA	NA	NA	NA	NA	NA	NA	NA	Most probably affecting splicing
RS1	c.326G>C	p.Gly109Ala	Tolerated	0.233	0.1812	Neutral	-0.86	NA	probably_damaging	1	Most probably affecting splicing
RS1	c.329G>A	p.Cys110Tyr	Tolerated	0.081	0.3342	Damaging	-2.69	0.5743	probably_damaging	0.93	Potential alteration of splicing
RS1	c.336_337delinsTT	p.Trp112_Leu113del	NA	NA	NA	NA	NA	NA	NA	NA	Potential alteration of splicing
RS1	c.337C>T	p.Leu113Phe	Tolerated	0.123	0.2754	Neutral	-1.98	NA	probably_damaging	0.99	Potential alteration of splicing
RS1	c.349C>T	p.Gln117*	NA	NA	NA	NA	NA	NA	NA	NA	Potential alteration of splicing
RS1	c.378del	p.Leu127*	NA	NA	NA	NA	NA	NA	NA	NA	Potential alteration of splicing
RS1	c.421C>T	p.Arg141Cys	Damaging	0.002	0.7215	Neutral	0.15	NA	probably_damaging	0.989	Significant alteration of exonic splicing enhancer / Exonic splicing silencer motifs ratio
RS1	c.422G>A	p.Arg141His	Damaging	0.033	0.4436	Neutral	-2.12	NA	probably_damaging	0.989	No significant impact on splicing signals
RS1	c.422G>T	p.Arg141Leu	Damaging	0.014	0.5317	Neutral	-2.26	NA	probably_damaging	0.97	No significant impact on splicing signals
RS1	c.435dup	p.Ile146AsnfsTer15	NA	NA	NA	NA	NA	NA	NA	NA	Significant alteration of exonic splicing enhancer / Exonic splicing silencer motifs ratio
RS1	c.438G>C	p.Glu146Asp	Tolerated	0.056	0.3819	Neutral	-1.38	NA	possibly_damaging	0.905	No significant impact on splicing signals
RS1	c.496_498del	p.Tyr166del	NA	NA	NA	NA	NA	NA	NA	NA	Significant alteration of exonic splicing enhancer / Exonic splicing silencer motifs ratio
RS1	c.496T>C	p.Tyr166His	Damaging	0.018	0.5068	Damaging	-3.96	0.7358	probably_damaging	0.998	No significant impact on splicing signals
RS1	c.498C>G	p.Tyr166*	NA	NA	NA	NA	NA	NA	NA	NA	Significant alteration of exonic splicing enhancer / Exonic splicing silencer motifs ratio
RS1	c.508A>C	p.Trp170Pro	Tolerated	0.082	0.3325	Damaging	-3.1	0.6355	probably_damaging	0.974	No significant impact on splicing signals
RS1	c.515del	p.Asn172Thrfs*95	NA	NA	NA	NA	NA	NA	NA	NA	Potential alteration of splicing
RS1	c.544C>T	p.Arg182Cys	Damaging	0.003	0.6824	Damaging	-3.86	0.7247	probably_damaging	0.999	Potential alteration of splicing
RS1	c.544C>A	p.Trp185Lys	Tolerated	0.105	0.2982	Neutral	-1.31	NA	possibly_damaging	0.806	Significant alteration of exonic splicing enhancer / Exonic splicing silencer motifs ratio
RS1	c.574_580delinsACCCCCCT	p.Pro192Thrfs*72	NA	NA	NA	NA	NA	NA	NA	NA	No significant impact on splicing signals
RS1	c.574C>T	p.Pro192Ser	Tolerated	0.149	0.2476	Damaging	-6.07	0.8987	probably_damaging	0.999	Significant alteration of exonic splicing enhancer / Exonic splicing silencer motifs ratio
RS1	c.575C>T	p.Pro192Leu	Damaging	0.045	0.4083	Damaging	-8.3	0.9698	probably_damaging	0.999	Significant alteration of exonic splicing enhancer / Exonic splicing silencer motifs ratio
RS1	c.577C>T	p.Pro193Ser	Damaging	0.033	0.4436	Damaging	-7.87	0.9611	probably_damaging	0.999	No significant impact on splicing signals
RS1	c.579dup	p.Ile194Hisfs*70	NA	NA	NA	NA	NA	NA	NA	NA	No significant impact on splicing signals
RS1	c.589C>T	p.Arg197Cys	Damaging	0	0.9125	Damaging	-7.83	0.96	probably_damaging	0.999	Significant alteration of exonic splicing enhancer / Exonic splicing silencer motifs ratio
RS1	c.590G>A	p.Arg197His	Damaging	0	0.9125	Damaging	-4.88	0.8135	probably_damaging	0.999	Potential alteration of splicing
RS1	c.596T>A	p.Ile199Asn	Damaging	0	0.9125	Damaging	-6.58	0.9196	probably_damaging	0.958	No significant impact on splicing signals
RS1	c.596T>C	p.Ile199Thr	Damaging	0.001	0.7849	Damaging	-4.38	0.7714	possibly_damaging	0.819	No significant impact on splicing signals
RS1	c.598C>T	p.Arg200Cys	Damaging	0	0.9125	Damaging	-7.87	0.9611	probably_damaging	0.999	No significant impact on splicing signals
RS1	c.598C>A	p.Arg200Ser	Damaging	0.001	0.7849	Damaging	-5.9	0.8884	probably_damaging	0.994	Potential alteration of splicing
RS1	c.599G>A	p.Arg200His	Damaging	0.001	0.7849	Damaging	-4.92	0.8167	probably_damaging	0.999	Significant alteration of exonic splicing enhancer / Exonic splicing silencer motifs ratio
RS1	c.608C>T	p.Pro203Leu	Damaging	0.023	0.4819	Damaging	-8.47	0.9725	probably_damaging	0.999	No significant impact on splicing signals
RS1	c.625C>T	p.Arg209Cys	Damaging	0.007	0.5993	Damaging	-3.25	0.6528	probably_damaging	0.999	No significant impact on splicing signals
RS1	c.637C>T	p.Arg213Trp	Damaging	0	0.9125	Damaging	-7.87	0.9611	probably_damaging	1	Significant alteration of exonic splicing enhancer / Exonic splicing silencer motifs ratio
RS1	c.638G>A	p.Arg213Gln	Damaging	0	0.9125	Damaging	-3.93	0.7327	probably_damaging	0.998	Significant alteration of exonic splicing enhancer / Exonic splicing silencer motifs ratio
RS1	c.647T>C	p.Leu216Pro	Damaging	0.029	0.4576	Damaging	-5.78	0.8799	probably_damaging	1	No significant impact on splicing signals
RS1	c.(?_1-1)_(52+1_53-1)del										
RS1	c.(184+1_185-1)_(522+1_523-1)del										
RS1	c.(52+1_53-1)_(184+1_185-1)del										
RS1	c.(52+1_53-1)_(78+1_79-1)del										

NA=not available.

Exonic deletions are described based on the edge positions of exons.

MutationTaster (<http://www.mutationtaster.org/>), FATHMM (<http://fathmm.biocompute.org.uk/>),SIFT (<https://www.sift.co.uk/>), PROVEAN (<http://provean.jcvi.org/index.php>),Polyphen 2 (<http://genetics.bwh.harvard.edu/pph2/>), Revel (<https://labworm.com/tool/revel>), CADD (<https://cadd.gs.washington.edu/info>),Human splicing finder, HSF (<http://www.umd.be/HSF3/>), ClinVar (<https://www.ncbi.nlm.nih.gov/clinvar/>).

Supplementary Table 6: Conservation Assessment

Gene	Nucleotide change	Amino acid change	Conservation				Conservation			
			PhyloP30way		PhastCons30way		PhyloP100way		PhastCons100way	
			Mammalian	Mammalian rankscore	Mammalian	Mammalian rankscore	vertebrate	vertebrate rankscore	vertebrate	vertebrate rankscore
RS1	c.20del	p.Gly7Alafs*119	NA	NA	NA	NA	NA	NA	NA	
RS1	c.35T>A	p.Leu12His	1.312	0.9471	1	0.8628	4.3379	0.5909	1	0.7164
RS1	c.52+1G>T		1.026	0.4595	1	0.8628	3.673	0.5433	1	0.7164
RS1	c.52+2T>C		1.026	0.4595	1	0.8628	3.673	0.5433	1	0.7164
RS1	c.52+5G>C		1.312	0.9471	1	0.8628	4.3379	0.5909	1	0.7164
RS1	c.53-34A>G		NA	NA	NA	NA	NA	NA	NA	NA
RS1	c.78G>C	p.Glu26Asp	0.9869	0.3637	0.9319	0.3999	3.026	0.4937	1	0.7164
RS1	c.103C>T	p.Gln35*	1.1759	0.7892	0.9819	0.4837	1.639	0.3679	1	0.7164
RS1	c.120C>A	p.Cys40*	-1.7869	0.008779	0.675	0.3039	-1.9049	0.01683	0.004	0.1661
RS1	c.184+2T>G		1.312	0.9471	0.981	0.4801	5.9429	0.6992	1	0.7164
RS1	c.185-1G>A		1.026	0.4595	0.999	0.7043	7.565	0.8134	1	0.7164
RS1	c.206T>C	p.Leu69Pro	1.312	0.9471	1	0.8628	8.9429	0.9253	1	0.7164
RS1	c.209G>A	p.Gly70Asp	1.026	0.4595	0.999	0.7043	7.565	0.8134	1	0.7164
RS1	c.214G>C	p.Glu72Gln	1.026	0.4595	0.9729	0.4571	7.565	0.8134	1	0.7164
RS1	c.214G>A	p.Glu72Lys	1.026	0.4595	0.9729	0.4571	7.565	0.8134	1	0.7164
RS1	c.216G>C	p.Glu72Asp	-0.708	0.03887	0.962	0.4353	1.159	0.3136	1	0.7164
RS1	c.239A>C	p.Gln80Pro	1.138	0.6469	1	0.8628	7.67	0.8291	1	0.7164
RS1	c.242T>A	p.Ile81Asn	1.312	0.9471	1	0.8628	8.9429	0.9253	1	0.7164
RS1	c.276G>C	p.Trp92Cys	1.026	0.4595	1	0.8628	7.565	0.8134	1	0.7164
RS1	c.288G>C	p.Trp96Cys	1.026	0.4595	1	0.8628	7.565	0.8134	1	0.7164
RS1	c.304C>T	p.Arg102Trp	0.2179	0.2429	0.998	0.6591	2.996	0.4914	1	0.7164
RS1	c.305G>A	p.Arg102Gln	1.026	0.4595	0.998	0.6591	7.565	0.8134	1	0.7164
RS1	c.308T>G	p.Leu103Arg	1.312	0.9471	1	0.8628	8.9429	0.9253	1	0.7164
RS1	c.317A>C	p.Gln106Pro	1.138	0.6469	1	0.8628	7.67	0.8291	1	0.7164
RS1	c.325G>C	p.Gly109Arg	1.026	0.4595	1	0.8628	7.565	0.8134	1	0.7164
RS1	c.325G>T	p.Gly109Trp	1.026	0.4595	1	0.8628	7.565	0.8134	1	0.7164
RS1	c.326+1G>A		1.026	0.4595	1	0.8628	7.565	0.8134	1	0.7164
RS1	c.326G>C	p.Gly109Ala	1.026	0.4595	1	0.8628	7.565	0.8134	1	0.7164
RS1	c.329G>A	p.Cys110Tyr	1.026	0.4595	0.98	0.4767	7.386	0.7904	1	0.7164
RS1	c.336_337delinsTT	p.Trp112_Leu113del	NA	NA	NA	NA	NA	NA	NA	NA
RS1	c.337C>T	p.Leu113Phe	1.1759	0.7892	1	0.8628	7.538	0.8096	1	0.7164
RS1	c.349C>T	p.Gln117*	1.1759	0.7892	0.9969	0.6203	9.371	0.9656	1	0.7164
RS1	c.378del	p.Leu127*	NA	NA	NA	NA	NA	NA	NA	NA
RS1	c.421C>T	p.Arg141Cys	1.1759	0.7892	0.998	0.6591	6	0.7034	1	0.7164
RS1	c.422G>A	p.Arg141His	1.026	0.4595	1	0.8628	7.32	0.7835	1	0.7164
RS1	c.422G>T	p.Arg141Leu	1.026	0.4595	1	0.8628	7.32	0.7835	1	0.7164
RS1	c.435dup	p.Ile146AsnfsTer15	NA	NA	NA	NA	NA	NA	NA	NA
RS1	c.438G>C	p.Glu146Asp	0.1289	0.1859	1	0.8628	0.6779	0.2496	0.999	0.4266
RS1	c.496_498del	p.Tyr166del	NA	NA	NA	NA	NA	NA	NA	NA
RS1	c.496T>C	p.Tyr166His	1.312	0.9471	1	0.8628	8.652	0.9084	1	0.7164
RS1	c.498C>G	p.Tyr166*	NA	NA	NA	NA	NA	NA	NA	NA
RS1	c.508A>C	p.Thr170Pro	1.138	0.6469	1	0.8628	7.4219	0.7941	1	0.7164
RS1	c.515del	p.Asn172Thrfs*65	NA	NA	NA	NA	NA	NA	NA	NA
RS1	c.544C>T	p.Arg182Cys	1.1759	0.7892	0.9459	0.4138	2.7739	0.4738	1	0.7164
RS1	c.554C>A	p.Thr185Lys	0.224	0.2485	0.985	0.4958	5.544	0.6694	1	0.7164
RS1	c.574_580delinsACCCCCCT	p.Pro192Thrfs*72	NA	NA	NA	NA	NA	NA	NA	NA
RS1	c.574C>T	p.Pro192Ser	1.1759	0.7892	0.998	0.6591	9.602	0.9762	1	0.7164
RS1	c.575C>T	p.Pro192Leu	1.1759	0.7892	0.999	0.7043	9.602	0.9762	1	0.7164
RS1	c.577C>T	p.Pro193Ser	1.1759	0.7892	1	0.8628	9.602	0.9762	1	0.7164
RS1	c.579dup	p.Ile194Hisfs*70	NA	NA	NA	NA	NA	NA	NA	NA
RS1	c.589C>T	p.Arg197Cys	1.1759	0.7892	1	0.8628	9.602	0.9762	1	0.7164
RS1	c.590G>A	p.Arg197His	1.026	0.4595	1	0.8628	7.565	0.8134	1	0.7164
RS1	c.596T>A	p.Ile199Asn	1.312	0.9471	0.998	0.6591	8.9469	0.9273	1	0.7164
RS1	c.596T>C	p.Ile199Thr	1.312	0.9471	0.998	0.6591	8.9469	0.9273	1	0.7164
RS1	c.598C>T	p.Arg200Cys	1.1759	0.7892	0.994	0.563	5.2989	0.6551	1	0.7164
RS1	c.598C>A	p.Arg200Ser	1.1759	0.7892	0.994	0.563	5.2989	0.6551	1	0.7164
RS1	c.599G>A	p.Arg200His	1.026	0.4595	0.9919	0.541	7.5679	0.8155	1	0.7164
RS1	c.608C>T	p.Pro203Leu	1.1759	0.7892	0.995	0.5772	9.602	0.9762	1	0.7164
RS1	c.625C>T	p.Arg209Cys	1.1759	0.7892	0.999	0.7043	7.7439	0.8394	1	0.7164
RS1	c.637C>T	p.Arg213Trp	1.1759	0.7892	1	0.8628	3.1719	0.5053	1	0.7164
RS1	c.638G>A	p.Arg213Gln	1.026	0.4595	1	0.8628	7.5679	0.8155	1	0.7164
RS1	c.647T>C	p.Leu216Pro	1.312	0.9471	1	0.8628	8.9469	0.9273	1	0.7164
RS1	c.(?_1-1)_(52+1_53-1)del									
RS1	c.(184+1_185-1)_(522+1_523-1)del									
RS1	c.(52+1_53-1)_(184+1_185-1)del									
RS1	c.(52+1_53-1)_(78+1_79-1)del									

NA=not available.

REFERENCES

- Ali A, Feroze AH, Rizvi ZH, Rehman TU. Consanguineous marriage resulting in homozygous occurrence of X-linked retinoschisis in girls. *Am J Ophthalmol* 2003 ;136 :767-769.
- Ambrosio L, Hansen RM, Kimia R, Fulton AB. Retinal function in X-linked juvenile retinoschisis. *Invest Ophthalmol Vis Sci* 2019;60:4872-4881.
- Andreoli MT, Lim JJ. Optical coherence tomography retinal thickness and volume measurements in X-linked retinoschisis. *Am J ophthalmol*. 2014;158:567-573.e3.
- Andreuzzi P, Fishman GA, Anderson RJ. Use of a carbonic anhydrase inhibitor in X-linked retinoschisis: effect on cystic-appearing macular lesions and visual acuity. *Retina* 2017;37:1555-61.
- Apushkin MA, Fishman GA, Janowicz MJ. Correlation of optical coherence tomography findings with visual acuity and macular lesions in patients with X-linked retinoschisis. *Ophthalmology* 2005;112:495-501.
- Apushkin MA, Fishman GA. Use of dorzolamide for patients with X-linked retinoschisis. *Retina*. 2006;26:741–5.
- Apushkin MA, Fishman GA, Rajagopalan AS. Fundus findings and longitudinal study of visual acuity loss in patients with X-linked retinoschisis. *Retina* 2005;25:612-618.
- Baumgartner S, Hofmann K, Chiquet-Ehrismann R, Bucher P. The discoidin domain family revisited: new members from prokaryotes and a homology-based fold prediction. *Protein Sci* 1998;7(7):1626-31.
- Byrne LC, Öztürk BE, Lee T, et al. Retinoschisin gene therapy in photoreceptors, Müller glia or all retinal cells in the *Rs1h*^{-/-} mouse. *Gen Ther* 2014;21:585-92.
- Bowles K, Cukras C, Turriff A, Sergeev Y, Vitale S, Bush RA, Sieving PA. X-Linked Retinoschisis: RS1 mutation severity and age affect the ERG phenotype in a cohort of 68 affected male subjects. *Invest Ophthalmol Vis Sci* 2011; 52:9250-6.
- Chen C, Xie Y, Sun T, et al. Clinical findings and RS1 genotype in 90 Chinese families with X-linked retinoschisis. *Molecular Vision* 2020;26:291-298.
- Chen J, Xu K, Zhang X, et al. Novel mutations of the RS1 gene in a cohort of Chinese families with X-linked retinoschisis. *Mol Vis* 2014;20:132-9.
- Collison FT, Genead MA, Fishman GA, Stone EM. Resolution of mid-peripheral schisis in x-linked retinoschisis with the use of dorzolamide. *Ophthalmic genet*. 2014;35:125-27.
- Cukras CA, Huryn LA, Jeffrey BG, et al. Analysis of anatomic and functional measures in X-linked retinoschisis. *Invest Ophthalmol Vis Sci*. 2018 59:2841-47.

- Cukras C, Wiley HE, Jeffrey BG, et al. Retinal AAV8-RS1 Gene therapy for X-linked retinoschisis: initial findings from a phase I/II Trial by Intravitreal Delivery. *Mol Ther* 2018 Sep 5;26(9):2282-2294.
- D'Souza L, Cukras C, Antolik C, Craig C, Lee J, He H, Li S, Smaoui N, Hejtmancik JF, Sieving PA, Wang X. Characterization of novel RS1 exonic deletions in juvenile X-linked retinoschisis. *Mol Vis* 2013; 19:2209-16. [PMID: 24227916].
- De Silva SR, Arno G, Robson AG, et al. The X-linked retinopathies: Physiological insights, pathogenic mechanisms, phenotypic features and novel therapies. *Prog Retin Eye Res* 2020:100898.
- Eksandh LC, Ponjavic V, Ayyagari R, Bingham EL, Hiriyantha KT, Andreasson S, et al. Phenotypic expression of juvenile X linked retinoschisis in Swedish families with different mutations in the XLR1 gene. *Arch Ophthalmol*. 2000;118:1098–104.
- Eriksson U, Larsson E, Holmstrom G. Optical coherence tomography in the diagnosis of juvenile X-linked retinoschisis. *Acta Ophthalmol Scand* 2004;82:218-223.
- Fahim AT, Ali N, Blachley T, Michaelides M. Peripheral fundus findings in X-linked retinoschisis. *Br J Ophthalmol* 2017;101:1555-1559.
- Gao FJ, Dong JH, Wang DD, et al. Comprehensive analysis of genetic and clinical characteristics of 30 patients with X-linked juvenile retinoschisis in China. *Acta Ophthalmol* 2020 Oct 30 doi: 10.1111/aos.14642. Online ahead of print.
- Genead MA, Fishman GA, Walia S. Efficacy of sustained topical dorzolamide therapy for cystic macular lesions in patients with X-linked retinoschisis. *Arch Ophthalmol*. 2010; 128:190-97.
- George ND, Yates JR, Moore AT. X linked retinoschisis. *Br J Ophthalmol*. 1995;79:697-702.
- George ND, Yates JR, Moore AT. Clinical features in affected males with X-linked retinoschisis. *Arch of ophthalmol* 1996;114:274-280.
- Gerth C, Zawadzki RJ, Werner JS, Heon E. Retinal morphological changes of patients with X-linked retinoschisis evaluated by Fourier-domain optical coherence tomography. *Arch Ophthalmol* 2008;126:807-811.
- Gliem M, Holz FG, Stohr H, Weber BH, Charbel Issa P. X-linked juvenile retinoschisis in a consanguineous family : phenotypic variability and report of a homozygous female patient. *Retina* 2014;34:2472-2478.
- Gregori NZ, Berrocal AM, Gregori G, et al. Macular spectral domain optical coherence tomography in patients with X-linked retinoschisis. *Br J ophthalmol* 2009 ;93 :373-378.
- Grigg JR, Hooper CY, Fraser CL, Cornish EE, McCluskey PJ, Jamieson RV. Outcome measures in juvenile X-linked retinoschisis: A systematic review. *Eye* 2020;34:1760-1769.

- Gurbaxani A, Wei M, Succar T, et al. Acetazolamide in retinoschisis: a prospective study. *Ophthalmology* 2014; 121:802-3 e3.
- Haas J. Über das Zusammen Vorkommen von Veränderungen der Retina und Choroidea. *Arch Augenheilkd.* 1898;37:343-348.
- Hinds AM, Fahim A, Moore AT, Wong SC, Michaelides M. Bullous X-linked retinoschisis: clinical features and prognosis. *Br J Ophthalmol* 2018;102:622-624.
- Jeffrey BG, Cukras CA, Vitale S, Turriff A, Bowles K, Sieving PA. Test-retest intervisit variability of functional and structural parameters in X-linked retinoschisis. *Transl Vis Sci Technol.* 2014;3:5.
- Kellner U, Brümmer S, Foerster MH, Wessing A. X-linked congenital retinoschisis. *Graefes Arch Clin Exp Ophthalmol.* 1990;228:432-437.
- Khandhadia S, Trump D, Menon G, Lotery AJ. X-linked retinoschisis maculopathy treated with topical dorzolamide, and relationship to genotype. *Eye* 2011;25:922–8.
- Kim DY, Mukai S. X-linked juvenile retinoschisis (XLRS): a review of genotype-phenotype relationships. *Semin Ophthalmol.* 2013;28:392–6.
- Kim LS, Seiple W, Fishman GA, Szlyk JP. Multifocal ERG findings in carriers of X-linked retinoschisis. *Doc Ophthalmol* 2007;114:21-26.
- Kjellström S, Vijayasarathy C, Ponjavic V, Sieving PA, Andréasson S. Long-term 12 year follow-up of X-linked congenital retinoschisis. *Ophthalmic Genet* 2010;31:114-125.
- Lesch B, Szabò V, Kánya M, et al. Clinical and genetic findings in Hungarian patients with X-linked juvenile retinoschisis. *Mol Vis* 2008;14:2321-2332.
- Ling KP, Mangalesh S, Tran-Viet D, et al. Handheld spectral domain optical coherence tomography findings of x-linked retinoschisis in early childhood. *Retina* 2019; 00:1-8.
- Manschot WA. Pathology of hereditary juvenile retinoschisis. *Arch Ophthalmol* 1972;88(2):131-138.
- McAnany JJ, Park JC, Collison FT, Fishman GA, Stone EM. Abnormal 8-Hz flicker electroretinograms in carrier of X-linked retinoschisis. *Documenta ophthalmologica. Adv in Ophth* 2016 ;133 :61-70.
- Menke MN, Feke GT, Hirose T. Effect of aging on macular features of X-linked retinoschisis assessed with optical coherence tomography. *Retina* 2011;31:1186-1192.
- Molday LL, Hicks D, Sauer CG, et al. Expression of X-linked retinoschisis protein RS1 in photoreceptor and bipolar cells. *Invest Ophthalmol Vis Sci* 2001;42(3):816-25.
- Molday RS, Kellner U, Weber BH. X-linked juvenile retinoschisis: clinical diagnosis, genetic analysis, and molecular mechanisms. *Prog Retin Eye Res* 2012;31(3):195-212.

- Orès R, Mohand-Said S, Dhaenens CM, et al. Phenotypic characteristics of a French cohort of patients with X-linked retinoschisis. *Ophthalmology* 2018;125:1587-96.
- Ou J, Vijayasathay C, Ziccardi L, et al. Synaptic pathology and therapeutic repair in adult retinoschisis mouse by AAV-RS1 transfer. *J Clin Invest* 2015;125(7):2891-903.
- Padròn-Pérez N, Català-Mora J, Díaz J, et al. Swept-source and optical coherence tomography angiography in patients with x-linked retinoschisis. *Eye (Lond)* 2018;32:707-15.
- Pennesi ME, Birch DG, Jayasundera KT, et al. Prospective evaluation of patients with X-linked retinoschisis during 18 months. *Invest Ophthalmol Vis Sci.* 2018;59:5941-56.
- Pimenides D, George ND, Yates JRW, Bradshaw K, Roberts SA, Moore AT, et al. X-linked retinoschisis: clinical phenotype and RS1 genotype in 86 UK patients. *J Med Genet.* 2005;42:e35.
- Rahman N, Georgiou M, Khan KN, Michaelides M. Macular dystrophies: clinical and imaging features, molecular genetics and therapeutic options. *Br J Ophthalmol* 2020;104(4):451-60.
- Reid SN, Yamashita C, Farber DB. Retinoschisin, a photoreceptor-secreted protein, and its interaction with bipolar and muller cells. *J Neurosci* 2003;23(14):6030-40.
- Reid SN, Akhmedov NB, Piriev NI, et al. The mouse X-linked juvenile retinoschisis cDNA: expression in photoreceptors. *Gene* 1999;227(2):257-66.
- Renner AB, Kellner U, Fiebig B, Cropp E, Foerster MH, Weber BH. ERG variability in X-linked congenital retinoschisis patients with mutations in the RS1 gene and the diagnostic importance of fundus autofluorescence and OCT. *Doc Ophthalmol* 2008; 116:97-109. [PMID: 17987333].
- Rentzsch P, Witten D, Cooper GM, et al. CADD: predicting the deleteriousness of variants throughout the human genome. *Nucleic Acids Research* 2018;47(D1):D886-D94.
- Richards S, Aziz N, Bale S, et al. Standards and guidelines for the interpretation of sequence variants: a joint consensus recommendation of the American College of Medical Genetics and Genomics and the Association for Molecular Pathology. *Genet Med* 2015;17(5):405-24.
- Riveiro-Alvarez R, Trujillo-Tiebas M-J, Gimenez-Pardo A, Garcia-Hoyos M, Lopez-Martinez M-A, Aguirre-Lamban J, et al. Correlation of genetic and clinical findings in Spanish patients with X-linked juvenile retinoschisis. *Invest Ophthalmol Vis Sci.* 2009;50:4342-50.
- Rodriguez FJ, Rodriguez A, Mnedoza-Londono R, Tamayo ML. X-linked retinoschisis in three females from the same family : a phenotype-genotype correlation. *Retina* 2005;25:69-74.
- Roesch MT, Ewing CC, Gibson AE, Weber BH. The natural history of X-linked retinoschisis. *Can J Ophthalmol* 1998;33:149-158.

- Saleheen D, Ali A, Khanum S, Ozair MZ, Zaidi M, Sethi MJ, Khan N, Frossard P. Molecular analysis of the XLR51 gene in 4 females affected by X-linked juvenile retinoschisis. *Can J Ophthalmol* 2008 ;43 :596-599.
- Sauer CG, Gehrig A, Warneke-Wittstock R, et al. Positional cloning of the gene associated with X-linked juvenile retinoschisis. *Nat Genet* 1997;17(2):164-70.
- Shi L, Jian K, Ko ML, et al. Retinoschisin, a new binding partner for L-type voltage-gated calcium channels in the retina. *J Biol Chem* 2009;284(6):3966-75.
- Shinoda K, Ishida S, Oguchi Y, Mashima Y. Clinical characteristics of 14 japanese patients with X-linked juvenile retinoschisis associated with XLR51 mutation. *Ophthalmic Genet.* 2000;21:171–80.
- Sieving PA; MacDonald IM, Chan S, et al. X-linked juvenile retinoschisis. In: Pagon RA, Adam MP, Ardinger HH, eds. *Gene reviews* ®. Seattle WA, 1993.
- Simonelli F, Cennamo G, Ziviello C, et al. Clinical features of X linked juvenile retinoschisis associated with new mutations in the XLR51 gene in Italian families. *Br J Ophthalmol* 2003;87:1130-1134.
- Testa F, Di Iorio V, Gallo B, et al. Carbonic anhydrase inhibitors in patients with x-linked retinoschisis: effects on macular morphology and function. *Ophthalmic Genetics*, 2019;40:3, 207-12.
- The Retinoschisis Consortium Functional implications of the spectrum of mutations found in 234 cases with X-linked juvenile retinoschisis. *Hum Mol Genet* 1998;7(7):1185-92.
- Thobani A, Fishman GA. The use of carbonic anhydrase inhibitors in the retreatment of cystic macular lesions in retinitis pigmentosa and X-linked retinoschisis. *Retina* 2011; 31:312-15.
- Tsang SH, Vaclavik V, Bird AC, Robson AG, Holder GE. Novel phenotypic and genotypic findings in X-linked retinoschisis. *Arch of Ophth* 2007;125:259-267.
- Verbakel SK, van de Ven JP, Le Blanc LM, et al. Carbonic anhydrase inhibitors for the treatment of cystic macular lesions in children with X-linked juvenile retinoschisis. *Invest Ophthalmol Vis Sci.* 2016;57:5134-47.
- Vincent A, Robson AG, Neveu MM, Wright GA, Moore AT, Webster AR, Holder GE. A phenotype-genotype correlation study of X-linked retinoschisis. *Ophthalmology* 2013;120(7):1454-1464.
- Walia S, Fishman GA, Molday RS, et al. Relation of response to treatment with dorzolamide in X-linked retinoschisis to the mechanism of functional loss in retinoschisis. *Am J Ophthalmol.* 2009;147(1):111-5e1.

- Wu WW, Wong JP, Kast J, Molday RS. RS1, a discoidin domain-containing retinal cell adhesion protein associated with X-linked retinoschisis, exists as a novel disulfide-linked octamer. *J Biol Chem* 2005;280(11):10721-30.
- Xiao Y, Liu X, Tang L, Wang X, Coursey TG, Guo X, et al. X linked retinoschisis: phenotypic variability in a chinese family. [Erratum appears in *Sci Rep.* 2016;6:21940 Note: Coursey, Terry [corrected to Coursey, Terry G]; PMID: 26960251]. *Sci Rep.* 2016;6:20118.
- Xu F, Xiang H, Jiang R, Dong F, Sui R. Phenotypic expression of X-linked retinoschisis in Chinese families with mutations in the RS1 gene. *Doc Ophthalmol.* 2011;123:21-7.
- Yang FP, Willyasti K, Leo SW. Topical brinzolamide for foveal schisis in juvenile retinoschisis. *J Aapos.* 2013;17:225-7.
- Yang HS, Lee JB, Yoon YH, Lee JY. Correlation between spectral-domain OCT findings and visual acuity in X-linked retinoschisis. *Invest Ophthalmol Vis Sci.* 2014;55:3029-36.
- Yanoff M, Kertesz Rahn E, Zimmerman LE. Histopathology of juvenile retinoschisis. *Arch Ophthalmol* 1968;79(1):49-53
- Yu J, Ni Y, Keane PA, et al. Foveomacular schisis in juvenile X-linked retinoschisis: an optical coherence tomography study. *Am J Ophthalmol* 2010;149:973-978.e2.

ACKNOWLEDGEMENTS

Immeasurable appreciation and deepest gratitude for the help and support are extended to the following people who have contributed in making this study possible.

I would like to express my sincere gratitude to my International Tutor Professor Michel Michaelides for the continuous support of my PhD study and research, for his patience, motivation, enthusiasm and great knowledge. His guidance helped me in all the time of research and writing of this thesis. I would like to thank him for his kindness to allowing me to attend his Laboratory at University College London, Institute of Ophthalmology and Moorfields Eye Hospital during my PhD course.

I would like to really thank Dr. Michalis Georgiou for his help, guidance, encouragement, valuable comments, suggestions and friendship. He has always been present and kind in supporting me in all the phases of the work, sharing his knowledge and helping in the analysis of data and its statistical computations.

I would like to thank Mr. Bishwanath Pal for his great teaching, support and kindness during this permanence and beautiful experience at UCL Institute of Ophthalmology and Moorfields Eye Hospital.

My sincere thanks and gratitude go to Professor Gianni Virgili, Professor Stanislao Rizzo, Prof. Fabrizio Giansanti and Dr. Andrea Sodi who gave me the great opportunity of spending my Phd abroad and who are representing for me a guide and an example of dedication to research in Ophthalmology and Neuroscience.

I would like to thank Professor Felicita Pedata, Coordinator of the PhD course.

I would like to thank Dr. Franchini, Dr. Grasso, Dr. Caporossi and Dr. Giacomelli to be great teachers and to be always present in this important period of my life.

I thank Dr. Vittoria Murro, Dr. Daniela Bacherini and Dr. Dario Mucciolo for their support and friendship.

I would like to thank also Xiao Liu, Yu Fujinami-Yokokawa, Yang Lizhu, and Kaoru Fujinami from the Laboratory of Visual Physiology, Division of Vision Research, National Institute of Sensory Organs, National Hospital Organization Tokyo Medical Center, Tokyo, and from the Department of Ophthalmology, Keio University School of Medicine, Tokyo, Japan for their help in the genetic analysis.

Last but not the least, I would like to thank my parents Grazia and Enzo, my sister Cecilia, my friend Ilaria T. who represented and currently represents an amazing and great friend and colleague during this beautiful experience, my friends Annalisa and Richard, Chiara C. fundamental in my life in London; Federica, Chiara L., Letizia, Silvia L., Ilaria B., Alda, Francesco, Rossana, Enrica, friends of a whole life; my Italian colleagues Iacopo F., Alice, Ruggero, my international colleagues and friends Pandelis, Lorenzo L., Ryan, Barsha, Sudha, Marcela, Sandra, Supawat and Hagar supporting me both in London and in Italy.